

# Endogenous Uncertainty\*

Andrea Carriero

Queen Mary, University of London  
a.carriero@qmul.ac.uk

Todd E. Clark

Federal Reserve Bank of Cleveland  
todd.clark@clev.frb.org

Massimiliano Marcellino

Bocconi University, IGIER and CEPR  
massimiliano.marcellino@unibocconi.it

This draft: March 2018

## Abstract

We show that macroeconomic uncertainty can be considered as exogenous when assessing its effects on the U.S. economy. Instead, financial uncertainty can at least in part arise as an endogenous response to some macroeconomic developments, and overlooking this channel leads to distortions in the estimated effects of financial uncertainty shocks on the economy. We obtain these empirical findings with an econometric model that simultaneously allows for contemporaneous effects of both uncertainty shocks on economic variables and of economic shocks on uncertainty. While the traditional econometric approaches do not allow us to simultaneously identify both of these transmission channels, we achieve identification by exploiting the heteroskedasticity of macroeconomic data. Methodologically, we develop a structural VAR with time-varying volatility in which one of the variables (the uncertainty measure) impacts both the mean and the variance of the other variables. We provide conditional posterior distributions for this model, which is a substantial extension of the popular leverage model of Jacquier, Polson, and Rossi (2004), and provide an MCMC algorithm for estimation.

*J.E.L. Classification:* C11, C32, D81, E32.

*Keywords:* Uncertainty, Endogeneity, Identification, Stochastic Volatility, Bayesian Methods

---

\*We gratefully acknowledge comments from Daniel Lewis, Helmut Lütkepohl, Davide Pettenuzzo, Giorgio Primiceri, Harald Uhlig, Molin Zhong, and seminar participants at the Federal Reserve Board. The views expressed herein are solely those of the authors and do not necessarily reflect the views of the Federal Reserve Bank of Cleveland or the Federal Reserve System.

# 1 Introduction

Starting from the seminal work of Bloom (2009), the business cycle relationship between uncertainty and output growth and the transmission mechanism from one to the other have received substantial attention in the literature; see Bloom (2014) for an exhaustive survey. Various measures of uncertainty have been put forward, and several efforts have been made to study the macroeconomic effects and broader importance of uncertainty shocks. A non-exhaustive list of studies in this area includes Bloom (2009), Bloom, et al. (2012), Bachmann, Elstner, and Sims (2013), Caggiano, Castelnuovo, and Groshenny (2014), Jurado, Ludvigson, and Ng (2015, JLN), Rossi and Sekhposyan (2015), Baker, Bloom, and Davis (2016), Shin and Zhong (2018), Basu and Bundick (2017), Carriero, Clark, and Marcellino (2017, CCM), Cesa-Bianchi, Pesaran, and Rebucci (2017), and Caldara, et al. (2016).

While the definitions and measurements of uncertainty differ in all these contributions, the common denominator in this line of research is the way in which the effects of uncertainty shocks are identified and assessed. Specifically, most econometric studies typically estimate the effects of uncertainty on economic variables by using structural VARs with some recursive identification scheme, which all inevitably assume some type of causal direction between uncertainty and economic variables. The assumption typically made is that uncertainty (be it macroeconomic or financial) is exogenous; i.e., it does not react contemporaneously to economic variables, while economic variables react contemporaneously to uncertainty.<sup>1</sup>

However, as is well known in the profession, recursive schemes have the advantage of simplicity of implementation and interpretation, but in some cases, they can be hard to defend as a credible identification strategy. This is particularly true when economists have very little a priori, generally accepted, and theoretically grounded reasons to believe that a specific recursive ordering is valid. The study of uncertainty shocks is such a case, since the existing evidence and economic wisdom make us unable to take a stand on the direction of the causality between uncertainty and economic variables such as GDP growth. In line with this reasoning, Ludvigson, Ma, and Ng (2018, LMN) pointed out that most of these previous results could be biased by an endogeneity problem, and using an identification procedure based on external information, they concluded that macro uncertainty is mostly endogenous; i.e., it mainly reacts to growth conditions rather than being an exogenous source of business cycle fluctuations, while financial uncertainty is mostly exogenous.

In this paper we show that macroeconomic uncertainty can be considered as mostly exogenous when assessing its effects on the U.S. economy. Instead, financial uncertainty can at least in part arise as an endogenous response to some macroeconomic developments, and

---

<sup>1</sup>Exogenous as used here and in the rest of the paper is not meant to mean strict exogeneity. Rather, we use it as shorthand for uncertainty being predetermined within the period.

overlooking this channel leads to a distorted estimate of the effects of financial uncertainty shocks on the economy. We obtain these empirical findings with an econometric model in which current and past values of uncertainty affect the current levels of economic variables, and uncertainty is in turn also affected by them contemporaneously.

We achieve identification by means of a novel procedure hinging on the time-varying volatility of macroeconomic variables. Differently from the approaches based on recursive schemes, our identification strategy permits both the causal channel going from uncertainty to the macroeconomy and the opposite causal channel going from the macroeconomy to uncertainty (which we will refer to as the “feedback channel”) to be potentially relevant and quantifiable.

The existing literature has indeed shown that both of these channels can be relevant. For example, the case has been made that uncertainty has effects on the economy through firms’ behavior. Firms’ behavior can be influenced by uncertainty for several reasons, e.g., because of the real option value of waiting before taking investment decisions (e.g., Bernanke (1983), McDonald and Siegel (1986)); because of the postponement of hiring and capital investment decisions (e.g., Leduc and Liu (2012), Bloom (2009), Bloom, et al. (2012)); and because of the interaction with financial frictions constraining firms’ decisions (e.g., Arellano, Bai, and Kehoe (2011), Gilchrist, Sim, and Zakrajsek (2014)). From the consumers’ side, the effects of uncertainty on the macroeconomy are possible via precautionary savings (e.g., Basu and Bundick (2017) and Fernandez-Villaverde, et al. (2011)). Equivalently, it is reasonable to conjecture that lower growth, typically associated with higher unemployment, tighter credit conditions, and larger volatility in financial markets, in turn can increase uncertainty. One of the first papers to stress the possible endogeneity of uncertainty is Bachmann, Elstner, and Sims (2013). Using an identification strategy in which uncertainty shocks have no long-run effects on aggregate economic activity, they find that the uncertainty shocks then also have no effects in the short run. Instead, various measures of uncertainty substantially increase after a negative shock to aggregate economic activity (see, e.g., Bachmann and Moscarini (2011) and Fajgelbaum, Schaal, and Taschereau-Dumouchel (2014)).

In our framework, identification is obtained by a particular heteroskedasticity structure in which the time-varying conditional variances of the variables are driven by an uncertainty measure plus a stochastic idiosyncratic component. In this sense, our identification method belongs to the heteroskedasticity-based identification tradition (see, e.g., Rigobon (2003), Sentana and Fiorentini (2001), and the review in Kilian and Lütkepohl (2017, chapter 14)). However, differently from this tradition, our methodology is based on modeling the conditional variances via stochastic volatility. This difference is nontrivial, because it allows much more flexibility in the evolution of the conditional variances than regime switching

or GARCH specifications, since the time-varying volatilities have their own shocks that are independent from the shocks hitting the level of the variables. As we shall see, the use of stochastic volatility also impacts the type and number of identifying restrictions, which are different from those implied by other heteroskedasticity-based identification methods.

It is also worth mentioning that the presence of stochastic volatility makes the errors of our model non-Gaussian, so that another way to interpret our identification procedure is that it exploits the information in higher-order moments, rather than only in the second moments as in traditional Gaussian VARs. In this sense, our approach also belongs to the strand of the literature on identification in non-Gaussian models; see, for example, Lanne, Meitz, and Saikkonen (2017).

Methodologically, the model developed in this paper is a structural VAR with time-varying volatility in which one of the variables (the uncertainty measure) impacts both the mean and the variance of the other variables. We provide conditional posterior distributions for this model, which is a substantial extension of the leverage model of Jacquier, Polson, and Rossi (2004), a widely used model in the finance literature. These distributions are nontrivial because, with respect to the model of Jacquier, Polson, and Rossi (2004), our model entails an additional layer of complication insofar as the stochastic volatility factor also enters the conditional mean of the process. The efficiency and reliability of the algorithm are established in Monte Carlo experiments with simulated data, prior to use with monthly and quarterly U.S. datasets.

Our empirical application, based on both monthly and quarterly U.S. data over the period 1960-2017, leads to three main findings. First, when allowing for the simultaneous feedback effect, shocks to macro and financial uncertainty have a depressive effect on output growth, investment, and consumption, in line with previous empirical studies such as JLN and CCM and the theoretical contributions mentioned above. Second, when looking at macro uncertainty, we find strong evidence that coefficients related to the feedback channel are close to zero, which means that treating macroeconomic uncertainty as exogenous is likely harmless. Third, we find that some of the coefficients measuring the feedback effect of macroeconomic variables on financial uncertainty are significantly different from zero, thereby indicating that financial uncertainty can be endogenous to some extent. This pattern is particularly evident in the monthly dataset, with variables such as consumer spending, inflation, industrial production, and the federal funds rate all featuring negative feedback coefficients, implying that an increase in these indicators leads to a reduction in financial uncertainty. The endogeneity of financial uncertainty is in contrast to the findings of LMN, who find less endogeneity in financial uncertainty with respect to macro uncertainty, but more in line with the treatment of financial indicators as “fast” variables that can react

contemporaneously to macroeconomic shocks; see, e.g., Bernanke, Boivin, and Elias (2005).

The paper is structured as follows. Section 2 presents the model and the identification approach. Section 3 develops the estimation algorithm. Section 4 provides an illustrative application and Monte Carlo experiments based on a small-scale version of the model. Section 5 presents the main empirical results. Section 6 summarizes our main findings and concludes. The appendix contains derivations and algorithm diagnostics.

## 2 A model of endogenous uncertainty

### 2.1 Model specification

Our interest is in modeling the relationship between a set of economic variables, which we collect in the  $n$ -dimensional vector process  $y_t$ , and an observable scalar measure of uncertainty, which we label  $m_t$ .<sup>2</sup> We specify the following model:

$$y_t = \Pi_0 + \Pi_y(L)y_{t-1} + \Pi_m(L) \ln m_{t-1} + \phi \ln m_t + A^{-1} \Lambda_t^{0.5} \epsilon_t^* \quad (1)$$

$$\ln m_t = \alpha + \delta_y(L)y_{t-1} + \delta_m(L) \ln m_{t-1} + \psi \epsilon_t^* + \tilde{u}_t, \quad (2)$$

where  $\Pi_y(L)$  is an  $n \times n$  matrix polynomial,  $\Pi_m(L)$  is an  $n \times 1$  vector polynomial,  $\Pi_0$  and  $\phi$  are  $n \times 1$  vectors,  $\delta_y(L)$  and  $\delta_m(L)$  are  $1 \times n$  vector polynomials,  $\psi$  is a  $1 \times n$  vector, and  $\alpha$  is a scalar. The matrix  $A^{-1}$  is a lower triangular  $n \times n$  matrix with ones on the main diagonal, which describes the contemporaneous relationships across the economic variables, and  $\Lambda_t$  is an  $n \times n$  diagonal matrix. The shocks are  $\epsilon_t^* \sim iid N(0, I_n)$ ,  $\tilde{u}_t \sim iid N(0, \sigma_u^2)$ , and are mutually independent.

The model (1)-(2) is a structural VAR for the  $(n + 1)$ -dimensional vector  $(y_t' \ln m_t)'$ . There are three features that differentiate this model from the VARs typically used in the uncertainty literature (e.g., in studies such as Bloom (2009) and JLN).

The first major feature is that the model allows for bilateral simultaneity between economic variables and uncertainty. Specifically, the model allows for both i) the contemporaneous effects of a shock to uncertainty on the economic variables, as measured by  $\partial y_t / \partial \tilde{u}_t = \phi$ , and ii) the contemporaneous effect of a shock to economic variables on uncertainty, as measured by  $\partial \ln m_t / \partial \epsilon_t^* = \psi$  (we will refer to this as the “feedback effect”). This bilateral simultaneity is typically not present in the traditional implementations of uncertainty VARs, and is in general not achievable within the class of Gaussian models, since the

---

<sup>2</sup>The uncertainty measure could also be treated as unobservable. In this case, an additional step in the MCMC sampler would be needed in order to draw from its conditional posterior distribution. For an example of this approach in a model that does not allow for endogenous uncertainty, see Carriero, Clark, and Marcellino (2017).

number of reduced-form coefficients available in such a class of models is insufficient to pin down all of the contemporaneous relations across variables.

The second major feature of the model proposed here is that the disturbance term to the first block of equations (i.e.,  $A^{-1}\Lambda_t^{0.5}\epsilon_t^*$ ) is heteroskedastic, as opposed to the large majority of uncertainty VARs which are specified as homoskedastic. The assumption of heteroskedasticity in a VAR of macroeconomic variables has overwhelming support in the recent literature (see, e.g., Chan and Eisenstat 2018), and many uncertainty measures are constructed on the basis of some variant of a time-varying volatility model (e.g., the measures put forward by JLN and LMN). Therefore, having a model featuring time-varying volatility is key in assessing the effects of uncertainty. In this paper we show that — besides providing a better description of the data — the assumption of heteroskedasticity allows us to simultaneously identify the coefficient vectors  $\phi$  and  $\psi$ . Indeed this assumption implies that the VAR is unconditionally not Gaussian, which provides additional identifying information in the form of additional reduced-form moments.

The third feature of the model is that the measure of uncertainty is allowed to impact not only the conditional mean of the economic variables but also their conditional variance. More specifically, we assume that uncertainty is a common factor influencing the time-varying volatilities of all of the variables in the system. This feature is embedded in our specification of the matrix  $\Lambda_t$ , which collects on the main diagonal the time-varying volatilities of the structural shocks to the economic variables. We assume a factor structure for these volatilities. Specifically the volatilities on the diagonal of  $\Lambda_t$  are defined as:

$$\lambda_{jt} = m_t h_{jt}, \quad j = 1, \dots, n, \quad (3)$$

where  $m_t$  is the measure of uncertainty (and is common to all the volatilities), and  $h_{jt}$  are idiosyncratic volatilities each following:

$$\ln h_{jt} = \alpha_j + \delta_j \ln h_{jt-1} + \tilde{\eta}_{jt}, \quad j = 1, \dots, n, \quad (4)$$

where  $\tilde{\eta}_{jt} \sim iid N(0, \sigma_{\tilde{\eta}_j}^2)$  is independent from  $\tilde{\eta}_{it}$ ,  $i \neq j$ ,  $\epsilon_t^*$ ,  $\tilde{u}_t$ . Therefore, the time-varying conditional variance of each variable is decomposed into a component common to all variables and given by the observable uncertainty measure  $m_t$ , plus a variable-specific, unobservable stochastic component, given by  $h_{jt}$ . Equations (2) and (4) are specified in logarithms, as is common in stochastic volatility models to implicitly implement non-negativity constraints, and imply that  $m_t$  and (the elements of)  $h_t$  have log-normal distributions. For future reference, we collect the  $h_{jt}$ 's in the  $n \times 1$  vector process  $h_t$ , and we define:

$$\Lambda_t = m_t H_t, \quad (5)$$

where  $H_t$  is a diagonal matrix with  $\text{diag}(H_t) = h_t$ .

At a first inspection, the model in (1)-(2) might look somewhat asymmetric, in the sense that while the first equation contains the contemporaneous value of uncertainty ( $\phi \ln m_t$ ) as a regressor, the second equation contains the shock to  $y_t$  ( $\psi \epsilon_t^*$ ) as a regressor. It is important to stress that this choice does not impact the key feature of the model, namely the simultaneity in the conditional means of  $y_t$  and  $\ln m_t$ . Indeed the model in (1)-(2) is obviously a reparameterization of a model in which both shocks  $\epsilon_t^*$  and  $\tilde{u}_t$  appear in both the equations for  $y_t$  and the equation for  $\ln m_t$ .<sup>3</sup> However, the parameterization of (1)-(2) greatly simplifies estimation, while having the level of  $y_t$  as a regressor in (2) would introduce a second channel of simultaneity between the conditional variance of  $y_t$  and  $\ln m_t$ . Such a model would be highly nonlinear, increasing substantially the computational complexity without providing any major insights into the simultaneity in the conditional means with respect to the specification in (1)-(2).

The model in (1)-(4) nests some other models that previously appeared in the literature. Setting  $n = 1$ ,  $H_t = I$ ,  $\phi = 0$  provides the model of Jacquier, Polson, and Rossi (2004). Setting  $\psi = 0$  provides the model of Carriero, Clark, and Marcellino (2017). Finally, setting  $\psi = 0$  and shutting down time variation in volatilities ( $\Lambda_t = \Lambda$ ) provides the homoskedastic VAR specification of Jurado, Ludvigson, and Ng (2015). All these contributions set either  $\phi$  or  $\psi$  to a vector of zeros. As we shall see in the next subsection, this is equivalent to achieving identification by means of a triangular recursive structure in which uncertainty is ordered first ( $\psi = 0$ ) or last ( $\phi = 0$ ) in a VAR.

## 2.2 Identification

In this section we illustrate our identification strategy. To fix the ideas, we start from an illustrative example based on a simple bivariate version of the model, which we describe in Section 2.2.1. Then, we generalize the discussion to the general model in Section 2.2.2.

### 2.2.1 An illustrative example

Consider the special case of the model defined by (1)-(4), with  $n = 1$ :

$$y_t = \Pi_0 + \Pi_y y_{t-1} + \Pi_m \ln m_{t-1} + \phi \ln m_t + \sqrt{m_t h_t} \epsilon_t^* \quad (6)$$

$$\ln m_t = \alpha + \delta_y y_{t-1} + \delta_m \ln m_{t-1} + \psi \epsilon_t^* + \tilde{u}_t \quad (7)$$

$$\ln h_t = \alpha_h + \delta_h \ln h_{t-1} + \tilde{\eta}_t, \quad (8)$$

---

<sup>3</sup>This can be easily seen by inserting the expression for  $\ln m_t$  shown in (2) into the right-hand side of (1), which provides a reduced-form representation in which both equations contain both shocks  $\epsilon_t^*$  and  $\tilde{u}_t$ .

with  $\epsilon_t^* \sim iid N(0, 1)$ ,  $\tilde{u}_t \sim iid N(0, \sigma_u^2)$ ,  $\tilde{\eta}_t \sim iid N(0, \sigma_\eta^2)$  mutually independent (structural) shocks. Here,  $y_t$  is a scalar economic variable of interest, for example, GDP growth, while  $m_t$  denotes an observable uncertainty measure. The conditional mean of  $y_t$  depends on the contemporaneous (log) uncertainty through the term  $\phi \ln m_t$ . Uncertainty is endogenous, as it depends on the contemporaneous value of  $y_t$  through the term  $\psi \epsilon_t^*$ . We now relate the simultaneous equation model (6)-(8) with a standard VAR and show how identification is achieved. To do so, first consider the simpler homoskedastic model obtained by replacing (6) with:

$$y_t = \Pi_y y_{t-1} + \Pi_m \ln m_{t-1} + \phi \ln m_t + \sqrt{\sigma_\epsilon^2} \epsilon_t^*, \quad (9)$$

which also makes equation (8) redundant. The heteroskedasticity from the shock to the first equation has been removed and this shock now has a fixed variance  $\sigma_\epsilon^2$ . We also disregarded the intercepts, as they are irrelevant to discussing identification.

We will now derive the reduced form of this simpler model. Using equation (9) we can derive an expression for  $\psi \epsilon_t^*$ :

$$\psi \epsilon_t^* = \psi \frac{1}{\sqrt{\sigma_\epsilon^2}} (y_t - \Pi_y y_{t-1} - \Pi_m \ln m_{t-1} - \phi \ln m_t), \quad (10)$$

which can be fed into equation (7) so that we can write the following system:

$$\begin{bmatrix} 1 & -\phi \\ -\frac{\psi}{\sqrt{\sigma_\epsilon^2}} & 1 + \frac{\psi\phi}{\sqrt{\sigma_\epsilon^2}} \end{bmatrix} \begin{pmatrix} y_t \\ \ln m_t \end{pmatrix} = \begin{bmatrix} \Pi_y & \Pi_m \\ \delta_y - \frac{\psi\Pi_y}{\sqrt{\sigma_\epsilon^2}} & \delta_m - \frac{\psi\Pi_m}{\sqrt{\sigma_\epsilon^2}} \end{bmatrix} \begin{pmatrix} y_{t-1} \\ \ln m_{t-1} \end{pmatrix} + \begin{pmatrix} \sqrt{\sigma_\epsilon^2} \epsilon_t^* \\ \tilde{u}_t \end{pmatrix}. \quad (11)$$

The system above is a simultaneous equation model of output and uncertainty. By inverting the matrix on the left-hand side of (11), we obtain the reduced form:

$$\begin{pmatrix} y_t \\ \ln m_t \end{pmatrix} = \begin{bmatrix} c_{11} & c_{21} \\ c_{12} & c_{22} \end{bmatrix} \begin{pmatrix} y_{t-1} \\ \ln m_{t-1} \end{pmatrix} + \begin{pmatrix} \epsilon_t \\ u_t \end{pmatrix}; \quad Var \begin{pmatrix} \epsilon_t \\ u_t \end{pmatrix} = \begin{bmatrix} \Sigma_{11} & \Sigma_{12} \\ \Sigma_{12} & \Sigma_{22} \end{bmatrix} \quad (12)$$

where:

$$\begin{bmatrix} c_{11} & c_{21} \\ c_{12} & c_{22} \end{bmatrix} = \begin{bmatrix} 1 + \phi \frac{\psi}{\sqrt{\sigma_\epsilon^2}} & \phi \\ \frac{\psi}{\sqrt{\sigma_\epsilon^2}} & 1 \end{bmatrix} \begin{bmatrix} \Pi_y & \Pi_m \\ \delta_y - \Pi_y \frac{\psi}{\sqrt{\sigma_\epsilon^2}} & \delta_m - \Pi_m \frac{\psi}{\sqrt{\sigma_\epsilon^2}} \end{bmatrix}, \quad (13)$$

and

$$\begin{bmatrix} \Sigma_{11} & \Sigma_{12} \\ \Sigma_{12} & \Sigma_{22} \end{bmatrix} = \begin{bmatrix} 1 + \phi \frac{\psi}{\sqrt{\sigma_\epsilon^2}} & \phi \\ \frac{\psi}{\sqrt{\sigma_\epsilon^2}} & 1 \end{bmatrix} \begin{bmatrix} \sigma_\epsilon^2 & 0 \\ 0 & \sigma_u^2 \end{bmatrix} \begin{bmatrix} 1 + \phi \frac{\psi}{\sqrt{\sigma_\epsilon^2}} & \frac{\psi}{\sqrt{\sigma_\epsilon^2}} \\ \phi & 1 \end{bmatrix}. \quad (14)$$

The reduced-form model contains 7 coefficients ( $c_{11}, c_{21}, c_{12}, c_{22}, \Sigma_{11}, \Sigma_{12}, \Sigma_{22}$ ), but there are 8 parameters in the structural form ( $\phi, \psi, \Pi_y, \Pi_m, \delta_y, \delta_m, \sigma_\epsilon^2, \sigma_u^2$ ); therefore, the model is not identified. In the standard approach, identification is usually achieved by setting  $\psi = 0$ , which gives exactly 7 coefficients in both the reduced and the structural form.



Instead, in model (6)-(7) identification is achieved because in place of  $\sigma_\epsilon^2$  the term  $m_t h_t$  appears, which can be treated as known since  $m_t$  is observable and  $h_t$  is separately identified through equation (8). In other words, substituting  $m_t h_t$  for  $\sigma_\epsilon^2$  in (13) allows us to estimate both  $\phi$  and  $\psi$ . Indeed — at any given time  $t$ — we have:

$$\begin{bmatrix} c_{11t} & c_{21t} \\ c_{12t} & c_{22t} \end{bmatrix} = \begin{bmatrix} 1 + \phi \frac{\psi}{\sqrt{m_t h_t}} & \phi \\ \frac{\psi}{\sqrt{m_t h_t}} & 1 \end{bmatrix} \begin{bmatrix} \Pi_y & \Pi_m \\ \delta_y - \Pi_y \frac{\psi}{\sqrt{m_t h_t}} & \delta_m - \Pi_m \frac{\psi}{\sqrt{m_t h_t}} \end{bmatrix} \quad (15)$$

$$\begin{bmatrix} \Sigma_{11t} & \Sigma_{12t} \\ \Sigma_{12t} & \Sigma_{22t} \end{bmatrix} = \begin{bmatrix} 1 + \phi \frac{\psi}{\sqrt{m_t h_t}} & \phi \\ \frac{\psi}{\sqrt{m_t h_t}} & 1 \end{bmatrix} \begin{bmatrix} m_t h_t & 0 \\ 0 & \sigma_u^2 \end{bmatrix} \begin{bmatrix} 1 + \phi \frac{\psi}{\sqrt{m_t h_t}} & \frac{\psi}{\sqrt{m_t h_t}} \\ \phi & 1 \end{bmatrix}, \quad (16)$$

which — for any fixed  $t$  — has 7 coefficients in both the reduced form and the structural form. Computing the products in the right-hand side of (15) and (16), and vectorizing these matrix equations by row, leads to the following system of equations:

$$\left\{ \begin{array}{l} c_{11} = \Pi_y + \phi \delta_y \\ c_{21} = \Pi_m + \phi \delta_m \\ c_{12} = \delta_y \\ c_{22} = \delta_m \\ \Sigma_{11t} = \phi^2 (\psi^2 + \sigma_u^2) + h_t m_t + 2\phi\psi\sqrt{m_t h_t} \\ \Sigma_{12t} = \phi(\psi^2 + \sigma_u^2) + \psi\sqrt{m_t h_t} \\ \Sigma_{22} = \psi^2 + \sigma_u^2 \end{array} \right. \quad (17)$$

Note that the parameters of the conditional means in the reduced form are not time-varying, while the reduced-form equation for  $y_t$  has time-varying conditional variance (and covariance), but such time variation is entirely driven by  $m_t$  and  $h_t$ . It follows that the solution for  $(\phi, \psi, \Pi_y, \Pi_m, \delta_y, \delta_m, \sigma_u^2)$  of the system in (17) is the same for any  $t$ . In order to find such a solution, first note that under knowledge of  $\phi$  one can obtain  $(\Pi_y, \Pi_m, \delta_y, \delta_m)$  using the first four equations of the system in (17). Similarly, under knowledge of  $\psi$  one can obtain  $\sigma_u^2$  by using the last equation. The last equation can also be substituted in the equations for  $\Sigma_{11t}$  and  $\Sigma_{12t}$ , and the problem reduces to solving:

$$\left\{ \begin{array}{l} \Sigma_{11t} = \phi^2 \Sigma_{22} + m_t h_t + 2\phi\psi\sqrt{m_t h_t} \\ \Sigma_{12t} = \phi \Sigma_{22} + \psi\sqrt{m_t h_t} \end{array} \right. \quad (18)$$

for  $\phi$  and  $\psi$ . To verify the existence of a unique local solution, we follow Hamilton (1994, p.334) and compute the Jacobian:

$$J = \begin{pmatrix} 2\phi\Sigma_{22} + 2\psi\sqrt{m_t h_t} & 2\phi\sqrt{m_t h_t} \\ \Sigma_{22} & \sqrt{m_t h_t} \end{pmatrix}. \quad (19)$$

Since  $|J| = 2\psi m_t h_t$ , it is  $\text{rank}(J) = 2$ , unless  $\psi = 0$ , but in this case we would have over-identification, as we would have  $\Sigma_{11t} = \phi^2 \sigma_u^2 + m_t h_t$ ,  $\Sigma_{12} = \phi \sigma_u^2$ ,  $\Sigma_{22} = \sigma_u^2$ , which would give  $\phi = \Sigma_{12}/\Sigma_{22}$  and  $\phi^2 = (\Sigma_{11t} - m_t h_t)/\sigma_u^2$ , which over-identifies  $\phi$ . Note that as  $|J| \neq 0$  unless  $\psi = 0$ , we actually have global identification.

The identifying information comes from the time-varying volatility term  $m_t h_t$ . Indeed, note that if instead of  $m_t h_t$  — which is identified by (and can be estimated through) the transition equation (8) — we had an unknown parameter  $\sigma_\epsilon^2$ , then the two-equation system in (18) would contain three unknowns and therefore the model would be unidentified.<sup>4</sup> To further clarify this point, suppose that  $\sigma_\eta^2 = 0$ . In this case,  $h_t$  will no longer be a random state variable, but rather it will be a fixed constant ( $h_t = h$  for any  $t$ ), and this will make this case similar to the standard one (that is, there is one more parameter to be estimated, the constant level of  $h_t$ , i.e.  $h$ ), and the model would again be unidentified. Hence, the question arises: why is the situation so different when  $\sigma_\eta^2 > 0$ ?

The intuition behind this result can be explained in two ways: by looking at either the conditional or the unconditional moments of the shocks. Starting with the intuition based on conditional moments, when  $\sigma_\eta^2 > 0$ , more moments become available from the reduced form, because time variation in  $h_t$  means that we have more reduced-form error-variance matrices (each corresponding to a different point in time  $t$ ). The simplest way to think about this is within the simple textbook example  $Bu_t = e_t$ , where  $e_t$  is the structural shock (with an identity variance matrix) and  $u_t$  the reduced-form shock, with variance  $\Sigma$ . The matrix  $B$  is a full matrix with ones on the main diagonal (for a normalization) describing the contemporaneous relationships among the variables. Since  $\Sigma$  has only  $n(n-1)/2$  free parameters, while  $B$  has  $n(n-1)$  free parameters, there is no identification. Now, let us assume we have two regimes: one in which  $\Sigma = \Sigma(h_1)$  and the second in which  $\Sigma = \Sigma(h_2)$ . This doubles the number of parameters we have from the reduced form, which become  $n(n-1)$ . Instead, the number of parameters in the  $B$  matrix remains  $n(n-1)$ , and therefore, the order condition for identification is satisfied.<sup>5</sup> This approach to identification makes the

---

<sup>4</sup>A version of the model with only  $h_t$  appearing in the conditional variance would be identified as well (it would be  $|J| = 2\psi h_t$ ). However, such a model would not allow for an impact of uncertainty on the conditional variance of  $y_t$ . Similarly, a version of the model with only  $m_t$  appearing in the conditional variance would be identified as well (it would be  $|J| = 2\psi m_t$ ). However, such a model would impose the rather strong assumption that the shocks to the first equation have variance exactly equal to the variable  $m_t$ . Using both  $m_t$  and  $h_t$  allows us to have a second moment effect of the uncertainty measure while avoiding misspecification.

<sup>5</sup>This argument is similar to that in Rigobon (2003), even though it is important to stress that in our approach  $h_t$  is a state variable and not a vector of parameters. As discussed below, this implies that we have a sequence of conditional variance matrices that are restricted by the fact that they must obey the laws of motion specified in (2) and (4).

implicit assumption that the contemporaneous relationships among the variables (those described by the matrix  $A$ ) are constant over time.

The intuition based on unconditional moments is related to Gaussianity. A Gaussian random variable is entirely defined by its first two moments (which are sufficient statistics). In the case of shocks, the first moment is 0 so we are left with the second moments (variances) only. The problem of identification precisely arises because the variance-covariance matrix of the Gaussian shocks has only  $n(n-1)/2$  free coefficients, which often are not enough to identify all the contemporaneous relations we would like to (which are typically  $n(n-1)$ ). Instead, a non-Gaussian random variable has many more moments, and these additional moments can provide the additional information one needs for identification. In the case at hand, if  $\sigma_{\eta}^2 = 0$ , then the shocks are Gaussian, and therefore, we have the identification problem. Instead, if  $\sigma_{\eta}^2 > 0$ , the shocks are not Gaussian (they are a mixture of Gaussians with mixture weights  $\sqrt{m_t h_t}$ ), and therefore, we have identification.

The previous discussion clarifies that our method belongs to the family of methods for heteroskedasticity-based identification, considered in papers such as Rigobon (2003), Sentana and Fiorentini (2001), and Lanne and Lütkepohl (2008).<sup>6</sup> The use of a continuously changing volatility is studied in a more general context by Lewis (2017), who also considers the case of heteroskedasticity of arbitrary and unknown form. Another related strand of research considers identification in non-Gaussian models; see, for example, Lanne, Meitz, and Saikkonen (2017).<sup>7</sup> Kilian and Lütkepohl (2017) provide an excellent survey.

There is, however, a key difference between our approach and those in the existing literature: our approach is based on stochastic volatility. This difference is not trivial, because the stochastic volatilities are state variables, driven by their own shocks rather than being either deterministic or driven by (functions of) the same shocks driving the variables in level. This adds flexibility to the model, and it has implications for identification. Indeed the number of additional restrictions provided by the presence of stochastic volatility is different from that in other heteroskedasticity-based approaches to identification. For example, consider the case in which  $h_t$  is not a state variable, but a parameter that can change across two regimes, so that the model can have only two alternative values for the error variance,  $\Sigma(h_1)$  and  $\Sigma(h_2)$ . Clearly, because of the reasoning made in the paragraphs above, this two-regime model would provide exact identification. If we were to extend this

---

<sup>6</sup>Angelini, Bacchiocchi, and Fanelli (2017) extend this approach to identify the effects of uncertainty shocks allowing for endogeneity. In line with our results, they find that the uncertainty shocks can be treated as exogenous.

<sup>7</sup>The Lanne, Meitz, and Saikkonen (2017) approach nests a number of other identification procedures based on conditional heteroskedasticity, including Normandin and Phaneuf (2004), Lanne, Lütkepohl, and Maciejowska (2010), and Lütkepohl and Netšunajev (2014).

approach to  $T$  regimes, we would have the sequence of error variances  $\Sigma(h_1), \dots, \Sigma(h_T)$  and this would obviously lead to over-identification. Instead, in our approach  $h_1, \dots, h_T$  are not (mutually independent) parameters that need to be estimated; they are state variables that must obey the laws of motion in (4). This implies that the model is just-identified.

Finally, our identification strategy differs from the procedure introduced by LMN. The latter complements the usual restrictions on the covariance matrix with additional restrictions on the identified shocks. These are “event constraints,” in the terminology of LMN, requiring the identified shocks to be coherent with economic reasoning when some extraordinary events happen, and “correlation constraints,” which restrict the identified uncertainty shocks to minimize their correlation with the stock market; see LMN for details.

### 2.2.2 Identification in the general model

The logic illustrated in Section 2.2.1 can be extended to the general multivariate case. Consider the reduced form associated with the general model (1)-(2):

$$\begin{pmatrix} y_t \\ \ln m_t \end{pmatrix} = \begin{bmatrix} C_{11} & C_{21} \\ C_{12} & C_{22} \end{bmatrix} \begin{pmatrix} y_{t-1} \\ \ln m_{t-1} \end{pmatrix} + \begin{pmatrix} \epsilon_t \\ u_t \end{pmatrix}$$

with:

$$Var \begin{pmatrix} \epsilon_t \\ u_t \end{pmatrix} = \begin{bmatrix} \Sigma_{11t} & \Sigma_{12t} \\ \Sigma_{12t} & \Sigma_{22t} \end{bmatrix}.$$

In the appendix we show that the reduced-form coefficients and the structural coefficients are related through the following equations:

$$\left\{ \begin{array}{l} C_{11} = \Pi_y + \kappa B \phi \delta_y \\ C_{21} = \Pi_m + \kappa B \phi \delta_m \\ C_{12} = \delta_y \\ C_{22} = \delta_m \\ \Sigma_{11t} = B \Sigma_{tr,t} \Sigma'_{tr,t} B' + \kappa^2 \sigma_u^2 B \phi \phi' B' \\ \Sigma_{12t} = B \Sigma_{tr,t} \psi' + \kappa \sigma_u^2 B \phi \\ \Sigma_{22} = \sigma_u^2 + \psi' \psi \end{array} \right. \quad (20)$$

where

$$\Sigma_{tr,t} = A^{-1} \Lambda_t^{0.5}, \quad B = (I_n - \phi \kappa \psi \Sigma_{tr,t}^{-1})^{-1}, \quad \kappa = (1 + \psi \Sigma_{tr,t}^{-1} \phi)^{-1}.$$

As in the bivariate case,  $\delta_y$  and  $\delta_m$  are immediately identified through  $C_{12}$  and  $C_{22}$ . Moreover, under knowledge of  $\Sigma_{tr,t}$ ,  $\psi$ , and  $\phi$ , the first two equations and the last equation in the system can be solved for  $\Pi_y$ ,  $\Pi_m$ , and  $\sigma_u^2$ . Therefore, we can reduce the system linking

reduced and structural coefficients to:

$$\begin{cases} \Sigma_{11t} = B\Sigma_{tr,t}\Sigma'_{tr,t}B' + \kappa^2\sigma_u^2B\phi\phi'B' \\ \Sigma_{12t} = B\Sigma_{tr,t}\psi' + \kappa\sigma_u^2B\phi \end{cases}, \quad (21)$$

which needs to be solved for  $\Sigma_{tr,t}$ ,  $\psi$  and  $\phi$ . Since  $\Sigma_{tr,t} = A^{-1}\Lambda_t$ , where  $\Lambda_t$  is identified and  $A$  contains a total of  $(n^2 - n)/2$  coefficients, the total number of structural coefficients we need to obtain is  $(n^2 - n)/2 + 2n = \frac{1}{2}n^2 + \frac{3}{2}n$ . The elements in the two matrices  $\Sigma_{11t}$  and  $\Sigma_{12t}$  are  $(n^2 + n)/2 + n = \frac{1}{2}n^2 + \frac{3}{2}n$ , and therefore the order condition for identification is satisfied.

We then turn to the issue of whether the rank condition for  $\psi$  and  $\phi$  is also satisfied. To address this issue, let us introduce the orthonormal matrix  $P$ , such that  $PP' = P'P = I$  and  $\Sigma_{tr,t}PP'\Sigma'_{tr,t} = \Sigma_t$ . Let  $\phi$  and  $\psi$  and  $\Sigma_{tr,t}$  be the solution of (21). Then of course they also solve:

$$\begin{cases} \Sigma_{11t} = B\Sigma_{tr,t}PP'\Sigma'_{tr,t}B' + \kappa^2\sigma_u^2B\phi\phi'B' \\ \Sigma_{12t} = B\Sigma_{tr,t}PP'\psi' + \kappa\sigma_u^2B\phi \\ B = (I_n - \phi\kappa\psi PP'\Sigma_{tr,t}^{-1})^{-1} \\ \kappa = (1 + \psi PP'\Sigma_{tr,t}^{-1}\phi)^{-1} \end{cases}. \quad (22)$$

If we now define  $\Sigma_{tr,t}P = \tilde{\Sigma}_{tr,t}$  and  $\psi P = \tilde{\psi}$ , then  $\tilde{\Sigma}_{tr,t}$  and  $\tilde{\psi}$  are the solutions of the rotated system. This means that the elements of the vector  $\phi$  do not change at the solution, while any rotation  $P$  of the elements in  $\psi$  is still a solution. This can be immediately seen also by simply noting that (a rotation of)  $\psi$  can be derived by projecting  $\ln m_t$  on (a rotation of)  $\epsilon_t^*$ .

Importantly, though, if one limits the possible identification schemes to recursive schemes with alternative variable orderings, then the only admissible rotation matrices  $P$  are permutation matrices.<sup>8</sup> This in turn implies that alternative orderings of the variables will only re-shuffle the elements of the vector  $\psi$ , which in the new ordering will become  $\tilde{\psi}$ , but will not change the impact response of  $\ln m_t$  to — say — a generic  $j$ -th macroeconomic shock

---

<sup>8</sup>This set of identification schemes coincides with the set of “triangular” VARs as defined by Rubio-Ramirez, Waggoner, and Zha (2010), Definition 6.

of interest  $\epsilon_{jt}^*$ .<sup>9,10</sup> Indeed, define the permuted error

$$\epsilon_t^{**} = P\epsilon_t^*,$$

which is the error of the permuted model:

$$y_t = \Pi_y(L)y_{t-1} + \Pi_m(L)\ln m_{t-1} + \phi \ln m_t + \Sigma_{tr,t}\epsilon_t^{**}, \quad (23)$$

$$\ln m_t = \delta_y(L)y_{t-1} + \delta_m(L)\ln m_{t-1} + \psi\epsilon_t^{**} + \tilde{u}_t, \quad (24)$$

where  $\psi\epsilon_t^{**} = \psi P\epsilon_t^* = \tilde{\psi}\epsilon_t^*$ . Let us say that the permutation moves the variable of interest from position  $j$  to position  $i$ ; that is, the  $i$ -th row of  $P$  is given by  $P_i = \mathbf{e}'_j$  where  $\mathbf{e}'_j$  is a basis row vector featuring a 1 in position  $j$ . This means that  $\epsilon_{it}^{**} = \mathbf{e}'_j\epsilon_t^* = \epsilon_{jt}^*$ . The value of  $\partial \ln m_t / \partial \epsilon_{jt}^*$  is obviously unchanged, and:

$$\psi_j = \frac{\partial \ln m_t}{\partial \epsilon_{jt}^*} = \frac{\partial \ln m_t}{\partial \epsilon_{it}^{**}} = \tilde{\psi}_i,$$

which means we could look at either the  $i$ -th element of  $\tilde{\psi}$  or the  $j$ -th element of  $\psi$  to find the (same) impulse response of interest.

A relevant qualification to the previous statement concerns the estimation stage. In fact, since priors are elicited separately for the elements of  $A$  and  $\Lambda_t$ , the implied prior for the error variance of the economic shocks (i.e.,  $A^{-1}\Lambda_t A^{-1'}$ ) will change when changing the equation ordering, and therefore, different orderings would result in different prior specifications and then, potentially, different joint posteriors. This problem is not specific to our model, but rather it is inherent to all stochastic volatility VARs using the specification  $A^{-1}\Lambda_t A^{-1'}$  for the error variance. As noted by Sims and Zha (1998) and Primiceri (2005), this problem is mitigated in the case (as the one considered in this paper) in which the covariances in  $A^{-1}$  do not vary with time, because the likelihood will quickly dominate the prior as the sample size increases.<sup>11</sup>

---

<sup>9</sup>This argument applies to the impact response of uncertainty to the macroeconomic shocks  $\epsilon_t^*$ , and the reason is that there are no zero restrictions on the vector of coefficients multiplying  $\epsilon_t^*$  in the equation for  $\ln m_t$  (i.e., the vector  $\psi$ ). This is similar to what happens to the last variable in a Cholesky scheme: also for such variables the ordering of the preceding variables is immaterial to the responses, precisely because the variable comes last in the recursive system. However, this of course does not mean that  $\ln m_t$  is being implicitly ordered last in our model, since this would also require imposing the condition  $\phi = 0$ .

<sup>10</sup>Instead the response of the macroeconomic variables  $y_t$  to the macroeconomic shocks  $\epsilon_t^*$  will of course change with different orderings in the usual way.

<sup>11</sup>This problem can be entirely avoided by eliciting a prior on the whole error variance matrix rather than on the individual elements of the matrices  $A$  and  $\Lambda_t$ ; see, for example, Shin and Zhong (2018) and Bognanni (2017). The online appendix of Carriero, Clark, and Marcellino (2018b) provides a discussion and some empirical results on this problem, which they label the ‘‘prior ordering problem.’’

### 3 Model estimation

In this section we describe the Markov Chain Monte Carlo (MCMC) algorithm for the estimation of the model in (1)-(4). The model is a structural VAR with time-varying volatility in which one of the regressors (the uncertainty measure) impacts both the mean and the variance of the others. This model nests as a special case the leverage model of Jacquier, Polson, and Rossi (2004). The conditional posterior distributions of this model are nontrivial because, with respect to the model of Jacquier, Polson, and Rossi (2004), our model entails an additional layer of complication insofar as the stochastic volatility factor also enters the conditional mean of the process. Next, Sections 3.2 and 3.3 discuss, respectively, the priors used in the empirical application and the computation of impulse response functions.

#### 3.1 MCMC algorithm

We collect the model coefficients in three sets. First,  $\theta_1$  groups all the coefficients of the  $y_t$  equation:  $\Pi_0, \phi, A, \Pi_y(L), \Pi_m(L)$ . Second,  $\theta_2$  groups all the coefficients of the uncertainty equation:  $\alpha, \delta_y(L), \delta_m(L), \psi, \sigma_u^2$ . Third,  $\theta_3$  groups all the coefficients of the latent volatility processes:  $\alpha_j, \delta_j, \sigma_{\tilde{\eta}_j}^2, j = 1, \dots, n$ . The vector  $\theta$  contains  $\theta_1, \theta_2$  and  $\theta_3$ . Both  $y_t$  and  $m_t$  are observable, while  $h_t$  is a vector of state variables.

The data density of data and states is given by:

$$\begin{aligned} p(y_t, m_t, h_t | \theta) &= m_t^{-1-0.5n} \prod_{j=1}^n h_{jt}^{-1.5} \times p_G(\epsilon_t^*, \tilde{u}_t, \tilde{\eta}_t) \\ &= \underbrace{m_t^{-1-0.5n} \prod_{j=1}^n h_{jt}^{-1.5} p_G(\epsilon_t^*)}_{\text{eq. (1)}} \times \underbrace{p_G(\tilde{u}_t)}_{\text{eq. (2)}} \times \underbrace{p_G(\tilde{\eta}_t)}_{\text{eq. (4)}}, \end{aligned} \quad (25)$$

where it is clear which pieces are coming from equations (1), (2), and (4). A derivation can be found in the appendix. The data density (25) will be the basis of a Gibbs sampler that will draw from:

1.  $\mathbf{h}_{1:T} | \theta, \mathbf{y}_{1:T}, \mathbf{m}_{1:T}$
2.  $\theta | \mathbf{h}_{1:T}, \mathbf{y}_{1:T}, \mathbf{m}_{1:T}$ ,

where  $\mathbf{h}_{1:T}$ ,  $\mathbf{y}_{1:T}$ , and  $\mathbf{m}_{1:T}$  are the matrices containing the states and variables for  $t = 1, \dots, T$ . Step (2) of the algorithm will be further partitioned into three blocks:

- 2a  $\theta_1 | \theta_2, \theta_3, \mathbf{h}_{1:T}, \mathbf{y}_{1:T}, \mathbf{m}_{1:T}$ ,
- 2b  $\theta_2 | \theta_1, \theta_3, \mathbf{h}_{1:T}, \mathbf{y}_{1:T}, \mathbf{m}_{1:T}$ ,
- 2c  $\theta_3 | \theta_1, \theta_2, \mathbf{h}_{1:T}, \mathbf{y}_{1:T}, \mathbf{m}_{1:T}$ .

While steps (2b) and (2c) are straightforward, step (1) and step (2a) are nontrivial due to the simultaneity inherent in our model. We now proceed to analyze these steps in more detail.

### 3.1.1 Drawing $\mathbf{h}_{1:T}|\theta, \mathbf{y}_{1:T}, \mathbf{m}_{1:T}$

Under the assumption that the processes  $h_{jt}$  are idiosyncratic volatilities with independent shocks  $\tilde{\eta}_{it}$ , the density  $p(h_t|h_{t-1}, h_{t+1}, \theta, \mathbf{y}_{1:T}, \mathbf{m}_{1:T})$  can be decomposed into the product of  $\prod_{j=1}^n p(\mathbf{h}_{j1:T}|\theta, \mathbf{y}_{1:T}, \mathbf{m}_{1:T}, \mathbf{h}_{\neq j1:T})$  and drawn in blocks  $j = 1, \dots, n$ . The generic block  $\mathbf{h}_{j1:T}|\theta, \mathbf{y}_{1:T}, \mathbf{m}_{1:T}, \mathbf{h}_{\neq j1:T}$  is Markov and can be simulated via a sequence of:

$$\begin{aligned} & p(h_{jt}|h_{jt-1}, h_{jt+1}, \theta, \mathbf{y}_{1:T}, \mathbf{m}_{1:T}, \mathbf{h}_{\neq j1:T}) \\ \propto & h_{jt}^{-0.5} \exp\left(-\frac{e_{jt}^2}{2h_{jt}} \left[1 + \frac{\psi_j^2}{\sigma_u^2}\right] + \frac{e_{jt}}{\sqrt{h_{jt}}} \frac{\psi_j}{\sigma_u^2} [u_t - \psi_{\neq j} \epsilon_{\neq jt}^*]\right) \\ & \times h_{jt}^{-1} \exp\left(-\frac{(\ln h_{jt}^2 - \mu_{jt})^2}{\sigma_{\tilde{\eta}}^2}\right). \end{aligned} \quad (26)$$

The derivation of the conditional posterior in (26) is detailed in the appendix. Using an independence chain Metropolis step with the transition equation as proposal, i.e.,  $q \propto \exp(-(\ln h_t^2 - \mu_t)^2 / \sigma_{\tilde{\eta}}^2)$ ,<sup>12</sup> we can accept/reject with acceptance probability  $a = \min(1, \iota)$ , where

$$\iota = \frac{\frac{1}{\sqrt{h_{jt}^{cand}}} \exp\left(-\frac{e_t^2}{2h_{jt}^{cand}} \left[1 + \psi^2 / \sigma_u^2\right] + \frac{e_t}{\sqrt{h_{jt}^{cand}}} \frac{\psi_j}{\sigma_u^2} [u_t - \psi_{\neq j} \epsilon_{\neq jt}^*]\right)}{\frac{1}{\sqrt{h_{jt}^{pres}}} \exp\left(-\frac{e_t^2}{2h_{jt}^{pres}} \left[1 + \psi^2 / \sigma_u^2\right] + \frac{e_t}{\sqrt{h_{jt}^{pres}}} \frac{\psi_j}{\sigma_u^2} [u_t - \psi_{\neq j} \epsilon_{\neq jt}^*]\right)}. \quad (27)$$

### 3.1.2 Drawing $\theta|\mathbf{h}_{1:T}, \mathbf{y}_{1:T}, \mathbf{m}_{1:T}$

Consider again the kernel in (25), which depends on  $\epsilon_t^*$ ,  $\tilde{u}_t$ , and  $\tilde{\eta}_{jt}$ , where:

$$\epsilon_t^* = m_t^{-0.5} H_t^{-0.5} A(y_t - \Pi_0 - \Pi_y(L)y_{t-1} - \Pi_m(L) \ln m_{t-1} - \phi \ln m_t) \quad (28)$$

$$\tilde{u}_t = \ln m_t - \alpha - \delta_y(L)y_{t-1} - \delta_m(L) \ln m_{t-1} - \psi \epsilon_t^* \quad (29)$$

$$\tilde{\eta}_{jt} = \ln h_{jt} - \alpha_j - \delta_j \ln h_{jt-1}, \quad j = 1, \dots, n. \quad (30)$$

We need to express (25) as a function of the data, the states, and the coefficients  $\theta$  only (i.e., there must be no unobservable shocks). We can derive an expression for the first equation coefficients  $\theta_1$  by using (28). An expression for the second equation coefficients  $\theta_2$  can also be derived using the expression for  $\tilde{u}_t$  in (29). However, this is not sufficient to get to an

<sup>12</sup>The proposal density is slightly different at the beginning and the end of the sample.



expression without any unobservable shocks appearing, because the term  $\psi\epsilon_t^*$  would still be there, and therefore a further substitution for  $\epsilon_t^*$  using (28) is required. This happens because, conditional on  $\theta_2$ , the shock  $u_t$  is observable, but the shock  $\tilde{u}_t = u_t - \psi\epsilon_t^*$  is not observable. These considerations lead to:

$$p(y_t, m_t, h_t | \theta) = m_t^{-1-0.5n} \prod_{j=1}^n h_{jt}^{-1.5} \times \exp \left\{ -\frac{(y_t - \Pi X_t - \phi \ln m_t)' H_t^{-1} (y_t - \Pi X_t - \phi \ln m_t)}{2m_t} \right\} \quad (31)$$

$$\times \frac{1}{\sqrt{\sigma_u^2}} \exp \left\{ -\frac{1}{2\sigma_u^2} \left( \begin{array}{c} \ln m_t - \alpha - \delta_y(L)y_{t-1} - \delta_m(L) \ln m_{t-1} \\ -\psi m_t^{-0.5} H_t^{-0.5} (y_t - \Pi X_t - \phi \ln m_t) \end{array} \right)^2 \right\} \quad (32)$$

$$\times \prod_{j=1}^n \frac{1}{\sqrt{\sigma_{\eta_i}^2}} \exp \left\{ -\frac{(\ln h_{jt} - \alpha_j - \delta_j \ln h_{jt-1})^2}{2\sigma_{\eta_i}^2} \right\}, \quad (33)$$

where

$$\Pi X_t = \Pi_0 - \Pi_y(L)y_{t-1} - \Pi_m(L) \ln m_{t-1}.$$

Note that in the density above, the coefficients of the second equation,  $\theta_2$ , only appear in the kernel (32), and the coefficients of the third equation,  $\theta_3$ , only appear in the kernel (33). This means that — conditionally on  $\theta_1$  (and on the states and data) — (32) can be used as the posterior kernel for  $\theta_2$  and (33) as the posterior kernel for  $\theta_3$ .

In particular, since (32) is a Gaussian kernel, we have that  $\theta_2|y_t, m_t, h_t, \theta_1, \theta_3$  can be drawn via a Gibbs step based on using equation (2) as a linear regression model. Also, note that  $p(\theta_2|y_t, m_t, h_t, \theta_1, \theta_3) \propto p(\theta_2|y_t, m_t, h_t, \theta_1)$ . Similarly, since (33) is a (product of) inverse Gamma kernel(s), it follows that  $\theta_3|y_t, m_t, h_t, \theta_1, \theta_2$  can be drawn via a Gibbs step based on using equation (4) as a linear regression model. Also note that  $p(\theta_3|y_t, m_t, h_t, \theta_1, \theta_2) \propto p(\theta_3|h_t)$ .

We are now left with the coefficients  $\theta_1$ . These coefficients are challenging because — when  $\psi \neq 0$  — they appear in both (31) and (32). The posterior density  $p(\theta_1|y_t, m_t, h_t, \theta_1, \theta_2)$  is proportional to the product of the kernels (31) and (32):

$$p(\theta_1|y_t, m_t, h_t, \theta_2, \theta_3) \propto \frac{1}{\sqrt{\sigma_u^2}} \times \exp \left\{ -\frac{(y_t - \Pi X_t - \phi \ln m_t)' H_t^{-1} (y_t - \Pi X_t - \phi \ln m_t)}{2m_t} \right\} \times \exp \left\{ -\frac{1}{2\sigma_u^2} \left( \begin{array}{c} \ln m_t - \alpha - \delta_y y_{t-1} - \delta_m \ln m_{t-1} \\ -\psi m_t^{-0.5} H_t^{-0.5} (y_t - \Pi X_t - \phi \ln m_t) \end{array} \right)^2 \right\} p(\theta_1), \quad (34)$$

which is not a known distribution. Therefore, this calls for a Random Walk Metropolis step

with acceptance probability

$$a = \min \left( 1, \frac{p(\theta_1^{cand} | \mathbf{y}_{1:T}, \mathbf{m}_{1:T}, \mathbf{h}_{1:T}, \theta_2, \theta_3)}{p(\theta_1^{pres} | \mathbf{y}_{1:T}, \mathbf{m}_{1:T}, \mathbf{h}_{1:T}, \theta_2, \theta_3)} \right). \quad (35)$$

### 3.1.3 Efficiency and convergence of the algorithm

We have verified the properties of the estimation algorithm in our empirical applications. Figure 13 in Appendix 7.4 reports a summary set of diagnostics that all support convergence and good mixing of the MCMC algorithm. Section 4 further tests the algorithm using simulated data.

## 3.2 Priors

In the empirical application, we demean the variables and drop the intercepts, to reduce the dimensionality of the parameter space. The priors on all the coefficients of the equations for  $y_t$ ,  $\theta_1$ , are flat. For the equation for  $m_t$ , we elicit an independent Gaussian prior for each coefficient in the polynomials  $\delta_y(L)$  and  $\delta_m(L)$ , with standard deviation 1 and mean zero, with the only exception being the parameter associated with  $\ln m_{t-1}$  whose prior mean is set at 0.5. We assume a conjugate prior for  $\psi$  and  $\sigma_u^2$ , following Jacquier, Polson, and Rossi (2004), with  $\psi | \sigma_u^2 \sim N(0, \sigma_u^2 I_n)$  and  $\sigma_u^2 \sim IG(1 \times 0.05^2, 2)$ . Finally, for the equations for  $h_t$ , we elicit an independent Gaussian inverse gamma prior, with  $\delta_{h,j} \sim N(0.99, 0.1^2)$ ,  $\alpha_{h,j} \sim N(0, 0.1^2)$ ,  $j = 1, \dots, n$ , and  $\sigma_{\tilde{\eta}_i}^2 \sim IG(2 \times 0.005^2, 3)$ .

## 3.3 Impulse responses

We will use the model to compute the impulse response functions (IRFs) to an uncertainty shock of size  $\sqrt{\sigma_u^2}$ . Responses over a horizon of  $t+1, \dots, t+h$  are obtained by simulating the model under a baseline and a shocked scenario.

The baseline scenario is constructed as follows. Let  $i = 1, \dots, M$  be the index of the posterior draws from the MCMC algorithm. We generate  $M = 1000$  random paths of the shocks  $\epsilon_{t+1:t+h}^*$  and  $\tilde{\eta}_{jt+1:t+h}$ ,  $j = 1, \dots, n$ , by drawing from  $\epsilon_t^{*i} \sim iid N(0, 1)$  and  $\tilde{\eta}_{jt+1:t+h}^i \sim iid N(0, (\sigma_{\tilde{\eta}_j}^2)^i)$  where  $(\sigma_{\tilde{\eta}_j}^2)^i$  is the  $i$ -th draw from the simulated posterior of  $\sigma_{\tilde{\eta}_j}^2$ . Instead, the shock  $\tilde{u}_{t+1:t+h}$  is set to 0 in all of the  $M$  paths. As initial conditions, we set  $y_{t-1} = \ln m_{t-1} = 0$ . Then, for  $i = 1, \dots, M$  we can simulate the model:

$$y_t^i = \Pi_y^i y_{t-1}^i + \Pi_m^i \ln m_{t-1}^i + \phi^i \ln m_t^i + (A^{-1})^i \Lambda_t^{0.5, i} \epsilon_t^{*i} \quad (36)$$

$$\ln m_t^i = \delta_y^i y_{t-1}^i + \delta_m^i \ln m_{t-1}^i + \psi^i \epsilon_t^{*i} + \tilde{u}_t^i, \quad (37)$$

where  $\Lambda_t^{0.5, i}$  has diagonal entries  $m_t^{i0.5} h_{jt}^{i0.5}$ ,  $j = 1, \dots, n$ , and

$$\ln h_{jt}^i = \alpha_{h,j}^i + \delta_{h,j}^i \ln h_{jt-1}^i + \tilde{\eta}_{jt}^i, \quad j = 1, \dots, n. \quad (38)$$

The shocked scenario is built in the same way,<sup>13</sup> except that in all  $i = 1, \dots, M$  simulations we set  $\tilde{u}_{t+1:t+h} = (\sqrt{\sigma_u^2}; \mathbf{0}_{h-1 \times 1})'$ , i.e., an  $h$ -dimensional vector with all elements set to zero, with the exception of the first one, which is set to  $\sqrt{\sigma_u^2}$ .<sup>14</sup>

The generalized impulse response functions (GIRF) for each draw are then computed as the difference between the shocked and the baseline scenario:  $\left\{ y_{t,shocked}^i \right\}_{i=1}^M - \left\{ y_{t,baseline}^i \right\}_{i=1}^M$ .

## 4 Illustrative example and Monte Carlo evaluation

This section contains an illustrative application and a Monte Carlo evaluation based on the simple model (6)-(8). Empirical results based on the general model can be found in Section 5.

### 4.1 Illustrative empirical example

We start with evaluating empirically the relationship between GDP growth and uncertainty in the U.S. This relationship is interesting by itself and it has been studied in precedents such as Campbell, et al. (2001). We include it here partly for illustrative purposes, to help set ideas in a relatively simple framework.

We define  $y_t$  as the quarter-on-quarter GDP growth rate and  $\ln m_t$  as the JLN measure of macro uncertainty, with quarterly data ranging from 1960Q3 to 2017Q2. Details on the data and will be provided in Section 5.1. The posterior means of the parameters (with 5% and 95% percentiles in square brackets) are:

$$\begin{aligned}
 y_t = & \underbrace{\frac{2.3872}{[1.6239, 3.1101]}}_{\Pi_0} + \underbrace{\frac{0.2372}{[0.1270, 0.3446]}}_{\Pi_y} y_{t-1} + \underbrace{\frac{3.2571}{[0.3720, 6.8014]}}_{\Pi_m} \ln m_{t-1} \\
 & + \underbrace{\frac{-6.1050}{[-9.8013, -3.1023]}}_{\phi} \ln m_t + \sqrt{m_t h_t} \epsilon_t^* \\
 \ln m_t = & \underbrace{\frac{0.0449}{[0.0098, 0.0810]}}_{\alpha} + \underbrace{\frac{-0.0020}{[-0.0073, 0.0031]}}_{\delta_y} y_{t-1} + \underbrace{\frac{0.9341}{[0.8826, 0.9843]}}_{\delta_m} \ln m_{t-1} \\
 & + \underbrace{\frac{-0.0036}{[-0.0093, 0.0023]}}_{\psi} \epsilon_t^* + \tilde{u}_t; \quad \sigma_u^2 = \frac{0.0013}{[0.0011, 0.0015]}
 \end{aligned}$$

<sup>13</sup>Note that — importantly — this means that the sequences  $\epsilon_t^{*i}$  and  $\tilde{\eta}_{jt+1,t+h}^i$  used for the baseline case are also used for the alternative case.

<sup>14</sup>Since we are only evaluating first-order effects, it could also make sense to compute the responses shutting down the simulation of  $\epsilon_{t+1:t+h}^*$  and  $\tilde{\eta}_{jt+1,t+h}$ . The IRFs obtained by setting both  $\epsilon_{t+1:t+h}^* = 0$  and  $\tilde{\eta}_{jt+1,t+h} = 0$  are very similar to those obtained as described.

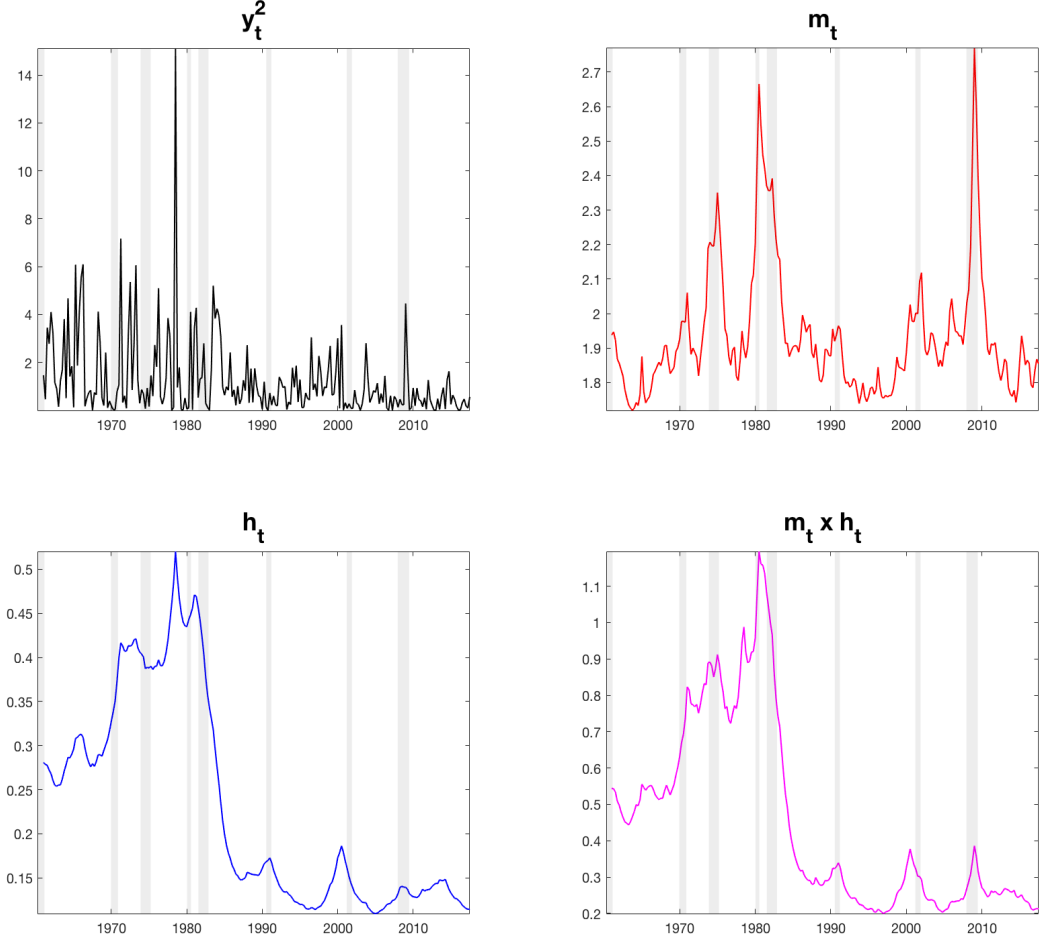


Figure 1: Squared GDP growth rates, uncertainty, idiosyncratic volatility states, and reduced-form volatilities.

$$\ln h_t = \underbrace{\frac{-0.0576}{[-0.1340, -0.0010]}}_{\alpha_h} + \underbrace{\frac{0.9653}{[0.9179, 1.0006]}}_{\delta_h} \ln h_{t-1} + \tilde{\eta}_t; \sigma_{\tilde{\eta}}^2 = \frac{0.0303}{[0.0112, 0.0636]}.$$

Therefore, the impact effect of uncertainty on growth as measured by  $\phi$  is negative, and also the effect of growth on uncertainty as measured by  $\psi$  is negative, but the value of zero is included in the 5-95% percentiles of the posterior of  $\psi$ .

Figure 1 reports the (exp of the) JLN uncertainty measure,  $m_t$ , the posterior mean of the latent state  $h_t$ , and the overall stochastic volatility term in the GDP growth equation,  $m_t h_t$ . The figure highlights the importance of having the  $h_t$  term, whose main roles are to further increase the volatility during the recessionary periods of the '70s and early '80s, and to capture the Great Moderation episode. Note that the overall conditional volatility of growth,  $m_t h_t$ , does not present a major peak in coincidence with the recent financial crisis.

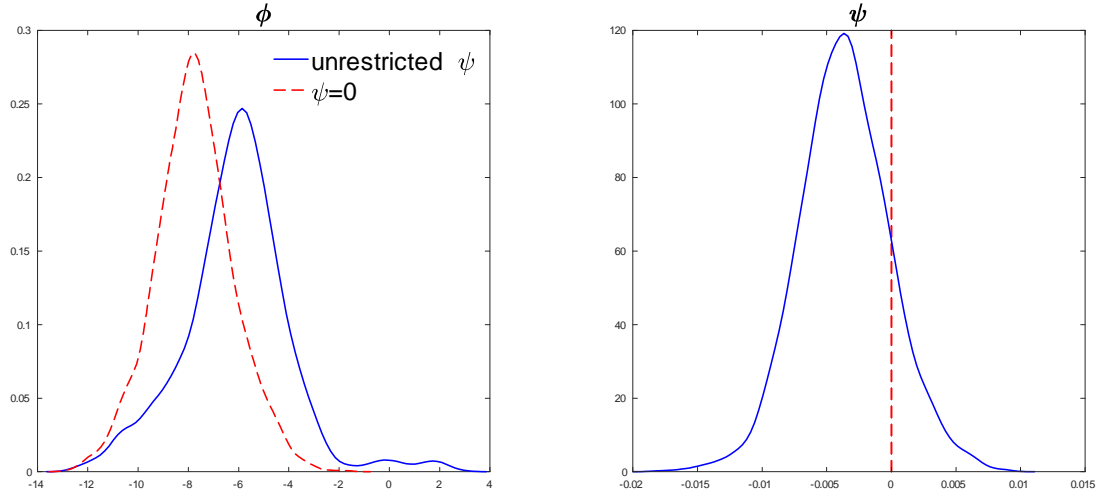


Figure 2: Posterior distributions of  $\phi$  and  $\psi$  when  $\psi$  is unrestricted (blue solid line) and when  $\psi$  is restricted to 0 (red dashed line). Model with JLN macro uncertainty.

This is in line with the behavior of the squared growth rates, also reported in Figure 1, and it is also partly due to the conditioning on  $m_t$ , and its lag, in the growth equation, which further dampens the conditional volatility of  $y_t$  during the crisis period.

We now focus on what would happen if we assumed exogeneity of uncertainty, in the sense of setting  $\psi = 0$ . The results become:

$$\begin{aligned}
 y_t &= \underbrace{\frac{2.4689}{[1.7293, 3.2063]}}_{\Pi_0} + \underbrace{\frac{0.2325}{[0.1242, 0.3410]}}_{\Pi_y} y_{t-1} + \underbrace{\frac{4.7887}{[2.0953, 7.5872]}}_{\Pi_m} \ln m_{t-1} \\
 &\quad + \underbrace{\frac{-7.7577}{[-10.3891, -5.0950]}}_{\phi} \ln m_t + \sqrt{m_t h_t} \epsilon_t^* \\
 \ln m_t &= \underbrace{\frac{0.0443}{[0.0098, 0.0809]}}_{\alpha} + \underbrace{\frac{-0.0019}{[-0.0071, -0.0032]}}_{\delta_y} y_{t-1} + \underbrace{\frac{0.9345}{[0.8828, 0.9844]}}_{\delta_m} \ln m_{t-1} \\
 &\quad + \underbrace{0}_{\psi} \epsilon_t^* + \tilde{u}_t; \sigma_{\tilde{u}}^2 = \frac{0.0013}{[0.0011, 0.0015]} \\
 \ln h_t &= \underbrace{\frac{-0.0591}{[-0.1363, -0.0015]}}_{\alpha_h} + \underbrace{\frac{0.9645}{[0.9160, 1.0005]}}_{\delta_h} \ln h_{t-1} + \tilde{\eta}_t; \sigma_{\tilde{\eta}}^2 = \frac{0.0302}{[0.0113, 0.0641]}
 \end{aligned}$$

Compared to the case with unrestricted  $\psi$ , the posterior of  $\phi$  shifts toward more negative values: the posterior mean goes from  $-6.1050$  to  $-7.7577$  (a decrease of 1.6527, more than 25%) and the 5%-95% range goes from  $[-9.8013, -3.1023]$  to  $[-10.3891, -5.0950]$ . Figure

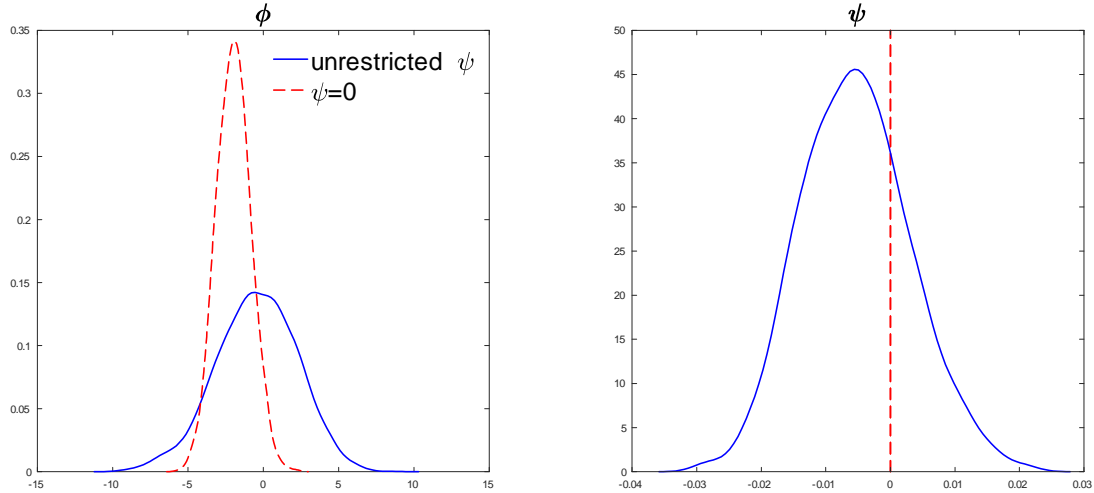


Figure 3: Posterior distributions of  $\phi$  and  $\psi$  when  $\psi$  is unrestricted (blue solid line) and when  $\psi$  is restricted to 0 (red dashed line). Model with VXO financial uncertainty.

2 shows the entire posterior distributions of  $\phi$  when  $\psi$  is either unrestricted or set to zero. Setting  $\psi = 0$  leads to an over-estimate of the negative impact of uncertainty on growth. This happens because, in the more general model with  $\psi \neq 0$ , following an uncertainty shock there is a decrease in growth, and this in turn increases uncertainty, which further decreases growth, increases uncertainty, and so on. If we shut down the feedback effect of growth on uncertainty by setting  $\psi = 0$ , the overall impact effect of uncertainty on growth, as measured by  $\phi$ , must increase (in absolute value).

Note also that, since the reduced-form parameter  $c_{21} = \Pi_m + \phi\delta_m$  in (17) cannot change, and  $\ln m_t$  and  $\ln m_{t-1}$  are highly correlated ( $\delta_m$  is about 0.93), to compensate for the distortion in  $\phi$ , the parameter  $\Pi_m$  increases by roughly the same amount of the decrease in  $\phi$ . Indeed, the median of the posterior of  $\Pi_m$  becomes much larger, increasing from 3.2571 to 4.7887 (by 1.5316), almost entirely offsetting the 1.6527 decrease in  $\phi$ . This means that the sum  $\phi + \Pi_m$  does not change much when imposing  $\psi = 0$ , and that under this restriction the model confounds the contemporaneous ( $\phi$ ) and the lagged effect ( $\Pi_m$ ) of uncertainty on growth.

Moreover, from the first equation of (17), the coefficient on lagged  $y$  in the equation for  $y$  is  $c_{11} = \Pi_y + \phi\delta_y$ . Since the product  $\phi\delta_y$  is very small, as  $\delta_y$  is very low relative to  $\phi$ , about  $-0.002$  versus  $-6.1050$ , the coefficient  $\Pi_y$  is virtually unaffected by the exclusion of the feedback channel. Finally, there are virtually no effects on the parameters of the equation for  $\ln m_t$  when setting  $\psi = 0$ . This is not attributable to the insignificance of  $\psi$  but rather is a consequence of the fact that  $\epsilon_t^*$  is uncorrelated with the other regressors, so

that its omission does not introduce a distortion.

To assess the bivariate relationship between GDP growth and financial (rather than macroeconomic) uncertainty, we now repeat the analysis using the Chicago Board Options Exchange (CBOE) S&P 100 Volatility Index, known as VXO, instead of the JLN measure of uncertainty, over the same sample, 1960Q3 to 2017Q2.

Figure 3 reports the entire posterior distributions of  $\phi$  and  $\psi$  under the two alternative cases  $\psi = 0$  and  $\psi \neq 0$  in the estimated model. Starting with the case  $\psi \neq 0$ , the distribution of  $\phi$  is centered around zero, which implies that financial uncertainty has virtually no effects on growth. As we shall see this result is likely due to omitted variables since it will change in the multivariate setting of Section 5. Setting  $\psi = 0$  shifts to the left the posterior distribution of  $\phi$ , and it also reduces its variance substantially. These results show that if financial uncertainty is treated as exogenous in this simple bivariate model, it can lead to an overestimation of its negative effects on growth, a result found for example in Campbell, et al. (2001), who suggested that the volatility of individual stock prices negatively co-moves with (detrended) GDP.

## 4.2 A Monte Carlo evaluation

The empirical results we have obtained with bivariate specifications lead us to conjecture that there can be an omitted variable bias in  $\phi$  when  $\psi$  is set at zero by mistake, though not a large one, but to confirm this statement we need a Monte Carlo evaluation where the true model is known. The Monte Carlo is also useful to evaluate the performance of the estimation algorithm.

We use the following data generating process (DGP) based on the model (6)-(8):

$$\begin{aligned}
 y_t &= \underbrace{0.1}_{\Pi_0} + \underbrace{0.25y_{t-1}}_{\Pi_y} - \underbrace{0.2 \ln m_{t-1}}_{\Pi_m} - \underbrace{0.25 \ln m_t}_{\phi} + m_t^{0.5} h_t^{0.5} \epsilon_t^* \\
 \ln m_t &= \underbrace{0}_{\alpha} + \underbrace{0.1 y_{t-1}}_{\delta_y} + \underbrace{0.95 \ln m_{t-1}}_{\delta_m} - \underbrace{0.55 \epsilon_t^*}_{\psi} + \tilde{u}_t; \sigma_{\tilde{u}}^2 = 0.05 \\
 \ln h_t &= \underbrace{0}_{\alpha_h} + \underbrace{0.999 \ln h_{t-1}}_{\delta_h} + \tilde{\eta}_t; \sigma_{\tilde{\eta}}^2 = 0.005
 \end{aligned}$$

With this DGP, we simulate 1000 time series for  $y_t$ ,  $m_t$ , and  $h_t$  with  $t = 1, \dots, 250$ . We then estimate the model in (6)-(8) with MCMC methods with 60,000 draws for each set of time series, and compute the average across replications of the mean of the posterior distribution for each parameter, together with the RMSE across replications.

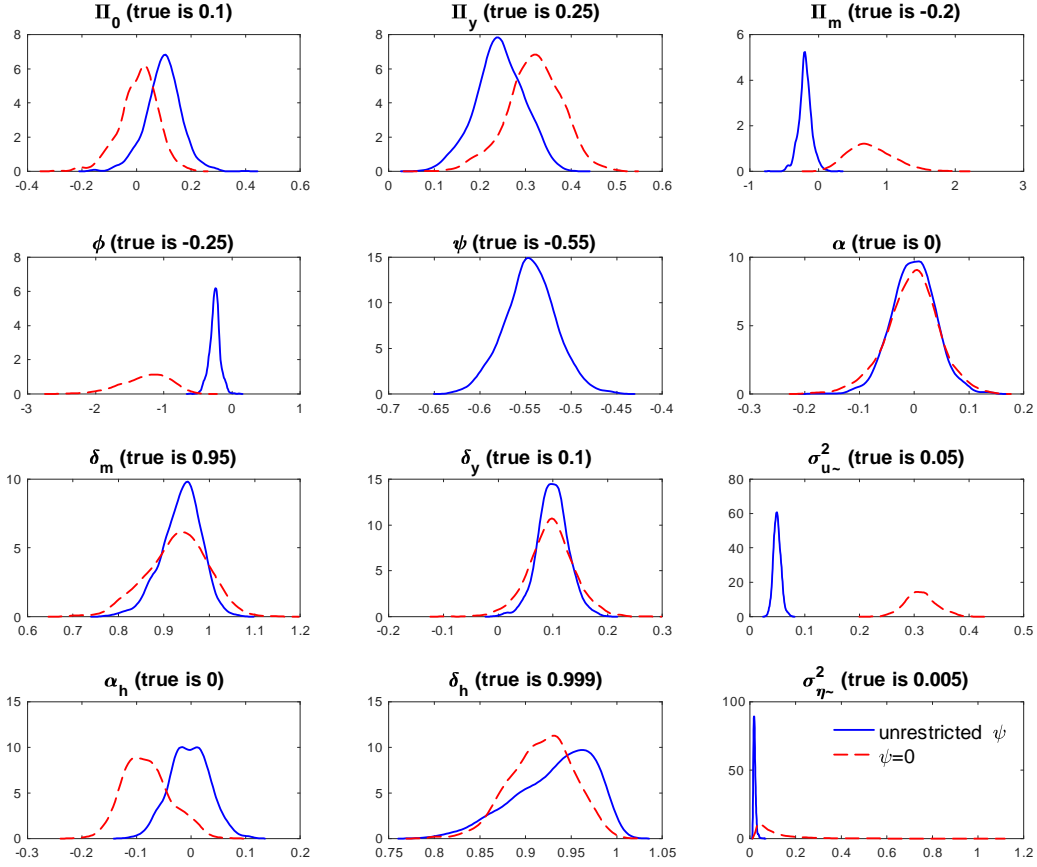


Figure 4: Monte Carlo results. Empirical distribution of the point estimates of the model coefficients across the Monte Carlo replications. Estimated model with  $\psi \neq 0$  and  $\psi = 0$ . DGP with  $\psi \neq 0$ .

Table 1. Monte Carlo results: effects of imposing  $\psi = 0$  when in the DGP  $\psi \neq 0$ .

	$\Pi_0$	$\Pi_y$	$\Pi_m$	$\phi$	$\psi$	$\alpha$	$\delta_m$	$\delta_y$	$\sigma_u^2$	$\alpha_h$	$\delta_h$	$\sigma_\eta^2$
DGP	0.1	0.25	-0.2	-0.25	-0.55	0	0.95	0.1	0.05	0	0.999	0.005
A: Unrestricted $\psi$												
Mean	0.098	0.244	-0.195	-0.253	-0.545	-0.001	0.938	0.100	0.050	-0.003	0.932	0.020
RMSE	0.066	0.053	0.097	0.077	0.028	0.040	0.045	0.028	0.007	0.036	0.079	0.016
B: $\psi = 0$												
Mean	0.007	0.320	0.766	-1.262	NaN	-0.004	0.929	0.097	0.312	-0.081	0.918	0.100
RMSE	0.117	0.092	1.021	1.070	NaN	0.049	0.069	0.042	0.263	0.091	0.088	0.123



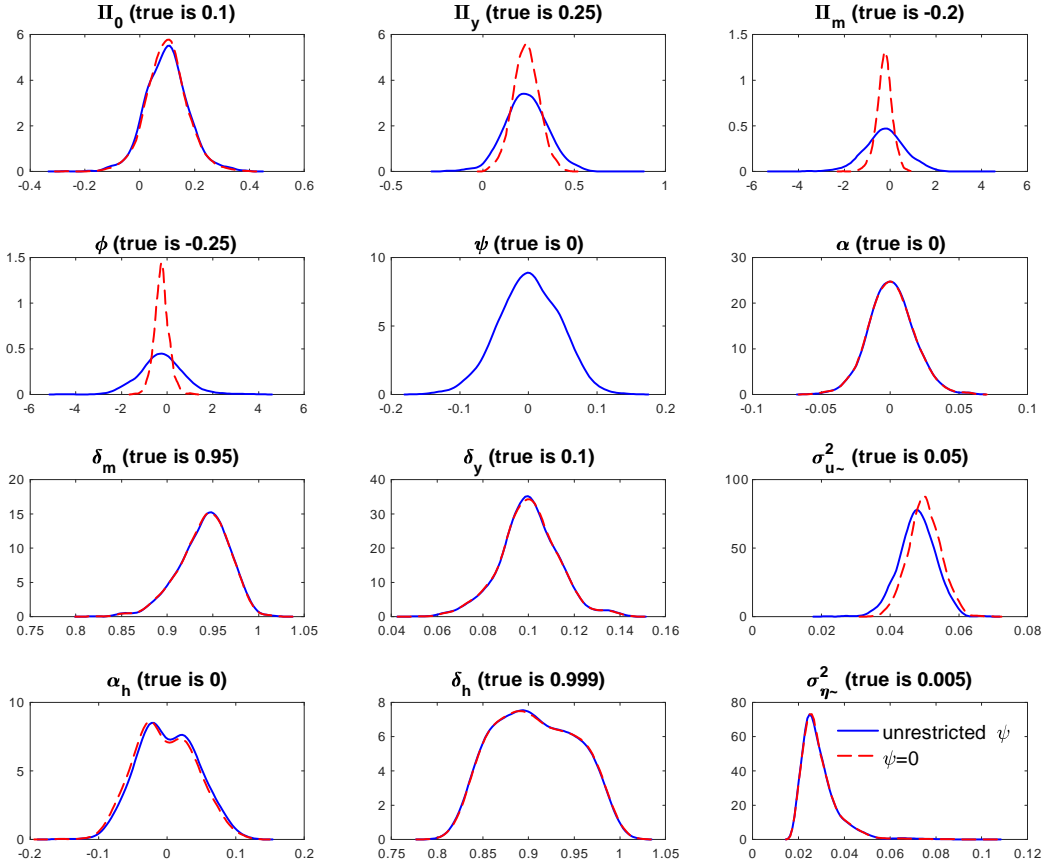


Figure 5: Monte Carlo results. Empirical distribution of the point estimates of the model coefficients across the Monte Carlo replications. Estimated model with  $\psi \neq 0$  and  $\psi = 0$ . DGP with  $\psi = 0$ .

Table 2. Monte Carlo results: effects of imposing  $\psi = 0$  when in the DGP  $\psi = 0$ .

	$\Pi_0$	$\Pi_y$	$\Pi_m$	$\phi$	$\psi$	$\alpha$	$\delta_m$	$\delta_y$	$\sigma_u^2$	$\alpha_h$	$\delta_h$	$\sigma_\eta^2$
DGP	0.1	0.25	-0.2	-0.25	0	0	0.95	0.1	0.05	0	0.999	0.005
A: Unrestricted $\psi$												
Mean	0.098	0.237	-0.235	-0.249	-0.55	0.001	0.940	0.100	0.048	0.001	0.907	0.029
RMSE	0.079	0.119	0.928	0.966	0.553	0.016	0.029	0.013	0.006	0.043	0.101	0.025
B: $\psi = 0$												
Mean	0.099	0.236	-0.246	-0.240	NaN	0.001	0.940	0.100	0.050	-0.003	0.908	0.029
RMSE	0.075	0.072	0.345	0.322	NaN	0.016	0.029	0.013	0.005	0.043	0.101	0.026

We start by considering a Monte Carlo design in which in the true DGP, the coefficient  $\psi$  is different from 0 (and specifically  $\psi = -0.55$ ), and the researcher either does or does not impose the restriction  $\psi = 0$ . The results for this MC design are shown in Table 1 and Figure 4. As is clear from panel A of Table 1, when the researcher chooses to leave the coefficient  $\psi$  unrestricted, the estimated model does not suffer from misspecification, and the resulting posterior densities are entirely in line with the true DGP. A similar conclusion can be drawn by looking at the empirical distributions of the point estimates of the coefficients across the Monte Carlo replications, which are drawn in blue in Figure 4.<sup>15</sup> These results also provide evidence of the effectiveness of the MCMC algorithm we use to simulate from the joint posterior of the model (which was described in Section 3)

However, if the researcher imposes the restriction  $\psi = 0$ , the resulting posterior distributions would be markedly distorted and would fail to recover the true values of the coefficients in the DGP. This can be seen in panel B of Table 1 and by an inspection of the empirical distributions of the point estimates in red in Figure 4. It is interesting to note that such distortions resemble the pattern we have found in the empirical application. Specifically, the posterior mean of the distribution of  $\phi$  moves from  $-0.253$  to  $-1.262$ , while that for  $\Pi_m$  shifts from  $-0.195$  to  $0.766$ , so that the sum  $\phi + \Pi_m$  is little changed, from  $-0.448$  to  $-0.496$ . As we have already emphasized, this is because the reduced-form parameter  $c_{21} = \Pi_m + \phi\delta_m$  in (17) cannot change, and — since  $\delta_m$  is equal to  $0.95$  — the parameter  $\Pi_m$  must increase by roughly the same amount of the decrease in  $\phi$ . There are no biases in the coefficients of the  $\ln m_t$  equation. However, the error variance of this equation (measured by  $\sigma_u^2$ ) becomes much larger when the restriction  $\psi = 0$  is imposed, which is a natural consequence of omitting the regressor  $\epsilon_t^*$  (this was not evident in the empirical application because in that case  $\psi$  was very small). Finally, imposing  $\psi = 0$  also has a distortionary effect on the estimated coefficients of all equations, as seen from the distributions reported in Figure 4.

Next, we consider a Monte Carlo design in which  $\psi = 0$  in the DGP. This means that there is no contemporaneous feedback effect of macro variables on uncertainty; that is, uncertainty is exogenous. As before, the researcher can either impose the restriction or not. This case resembles the case of redundant variables in the estimated model, which typically leads to inefficient — but yet unbiased — estimators. This is precisely what happens, as illustrated in Table 2 and Figure 5. In this case, both the model in panel A and that in panel B of the table recover the correct values for the coefficients, but the model in panel B attains more precise estimates, thanks to the fact that it imposes the correct restriction  $\psi = 0$ . The more general model leads to unbiased but inefficient estimates of the coefficients

---

<sup>15</sup>The point estimate for a given Monte Carlo replication is defined as the posterior mean of that replication.

of the first equation, because the steps of the sampler that draws these coefficients condition on the draws of  $\psi$ , which instead should be set to 0. This pattern can also be observed in Figure 5, where both the blue and red distributions are centered in the correct values for the coefficients, but the red distributions attain a smaller variance than the blue distributions. The coefficients of the second equation are not impacted, because the regressor to which  $\psi$  is attached is orthogonal to the other regressors in this equation. Finally, there is obviously no effect on the third equation.

Finally, we consider the effects of erroneously imposing the restriction  $\phi = 0$ , namely, no contemporaneous effects of uncertainty on  $y_t$ , while in the true DGP such a restriction does not hold. Results from this design are presented in Table 3 and Figure 6. The results in panel A of Table 3 show that by estimating the full model one can recover the true values of the coefficients.<sup>16</sup> Instead, as shown in panel B, imposing the restriction  $\phi = 0$  distorts the results. In particular, the contemporaneous effect of uncertainty on output (as measured by  $\phi$ ) is underestimated (set at  $\phi = 0$  rather than  $\phi = -0.25$ ), and since the reduced-form parameter  $c_{21} = \Pi_m + \phi\delta_m$  cannot change, the lagged effect  $\Pi_m$  gets over-estimated, by roughly  $-0.25$ . Moreover, the distortion in  $\phi$  implies a distortion in  $\epsilon_t^*$  (it no longer features zero mean), and therefore,  $\psi$  gets overestimated (in absolute value) and  $\sigma_u^2$  gets underestimated.

To conclude this section it is worth comparing the results obtained when imposing  $\phi = 0$  or  $\psi = 0$  under the DGP in which both of these parameters are nonzero, and relate them with identification. These are the results contained in panels B of Table 1 and Table 3 (and the respective graphs in Figures 4 and 6). The identification problem faced by the standard approach can be rephrased as follows. In the reduced form we have the parameter  $c_{21} = \Pi_m + \phi\delta_m$ , which is uniquely identified in the likelihood. Recursive identification schemes impose either  $\phi = 0$  or  $\psi = 0$ , which both amount to a potential omitted variable problem. We have that:

- If  $\psi = 0$  (uncertainty ordered first), then the estimated  $\phi$  will be more negative than it is in the DGP, and we have an overestimate of  $\Pi_m$ . In this case the identification scheme attributes too much of the impact variation to uncertainty and too little to lagged uncertainty.
- If  $\phi = 0$  (uncertainty ordered last), then the estimated  $\phi$  will be less negative than it is in the DGP, and we have an underestimate of  $\Pi_m$ . In this case the identification scheme attributes too little of impact variation to uncertainty and too much to lagged uncertainty.

---

<sup>16</sup>Note that these results coincide with those of panel A of Table 1, by construction.

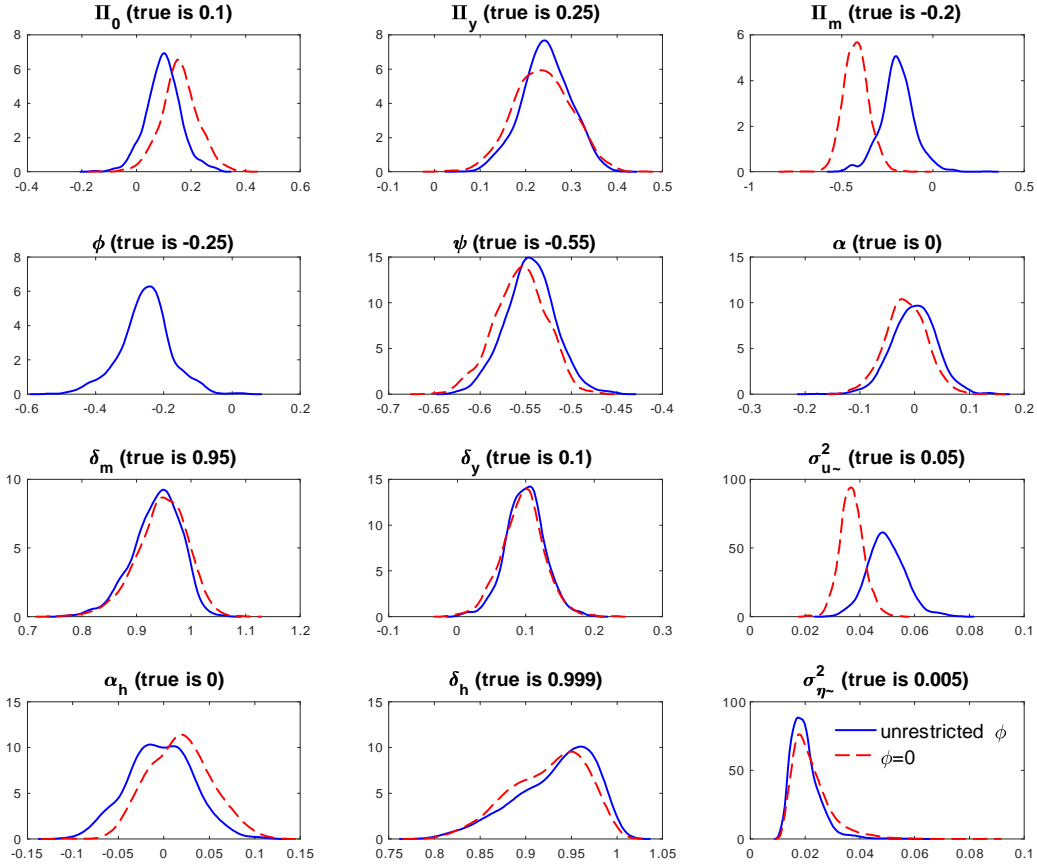


Figure 6: Monte Carlo results. Empirical distribution of the point estimates of the model coefficients across the Monte Carlo replications. Estimated model with  $\phi \neq 0$  and  $\phi = 0$ . DGP with  $\phi \neq 0$ .

Table 3. Monte Carlo results: effects of imposing  $\phi = 0$  when in the DGP  $\phi \neq 0$ .

	$\Pi_0$	$\Pi_y$	$\Pi_m$	$\phi$	$\psi$	$\alpha$	$\delta_m$	$\delta_y$	$\sigma_u^2$	$\alpha_h$	$\delta_h$	$\sigma_\eta^2$
DGP	0.1	0.25	-0.2	-0.25	-0.55	0	0.95	0.1	0.05	0	0.999	0.005
A: Unrestricted $\phi$												
Mean	0.098	0.244	-0.195	-0.253	-0.545	-0.001	0.938	0.100	0.050	-0.003	0.932	0.020
RMSE	0.066	0.053	0.097	0.077	0.028	0.040	0.045	0.028	0.007	0.036	0.079	0.016
B: $\phi=0$												
Mean	0.157	0.238	-0.420	NaN	-0.556	-0.016	0.946	0.096	0.037	0.018	0.923	0.022
RMSE	0.090	0.064	0.231	NaN	0.029	0.041	0.046	0.032	0.014	0.039	0.086	0.019

The approach we propose in this paper solves these issues, since it allows one to estimate a model for uncertainty and macroeconomic variables that does not put any restrictions on either  $\psi$  or  $\phi$ . The results of the Monte Carlo evaluation confirm the quality of the estimation algorithm, highlight the importance of properly modeling the endogeneity of uncertainty, and support the interpretation of the empirical findings about the relationship between GDP growth and either macro or financial uncertainty. In addition, there is no tendency to spuriously estimate a significant contemporaneous dependence of uncertainty on macro conditions when none exists in the DGP.

## 5 The economic effects of (endogenous) uncertainty

We now study the relationship between macroeconomic and financial uncertainty and economic variables. We do so using both quarterly and monthly data for the U.S. The data are described in Section 5.1. Section 5.2 provides the results of macro uncertainty shocks. Section 5.3 provides the results of financial uncertainty shocks. Section 5.4 provides a summary.

### 5.1 Data

To study the relationship between uncertainty and economic variables, we use two models, specified at different frequencies, since both monthly and quarterly data have been used in previous empirical analyses. We draw on commonly-used measures to capture macroeconomic uncertainty with the series of JLN, and financial uncertainty with the Chicago Board Options Exchange (CBOE) S&P 100 Volatility Index, known as VXO. In unreported results, we obtained similar results with the uncertainty measures of Carriero, Clark, and Marcellino (2017).

The first model is a VAR that includes seven quarterly indicators in addition to the uncertainty measure. We will refer to this model as the quarterly VAR. The variables included in the model are reported in Table 4.

The seven indicators are essentially those covered in the widely used DSGE model of Smets and Wouters (2007) and in many related analyses, such as Justiniano, Primiceri, and Tambalotti (2011). The set of indicators is also similar to that used by JLN (in their 8 variable VAR specification) to assess the effects of uncertainty shocks (setting  $\psi = 0$ ). We use four lags and the sample covers the period 1960Q3 to 2017Q2, for a total of  $T = 228$  observations. As mentioned, all variables are demeaned prior to estimation to reduce the computational burden. We obtained the raw macroeconomic data from the FAME database of the Federal Reserve Board of Governors. We obtained the JLN measure of uncertainty

from the website of Professor Ludvigson, defining our quarterly series as the within-quarter average of the source monthly series. To obtain the long series on the VXO measure, we followed the precedents of other studies in the literature and spliced realized volatility of S&P 500 returns (monthly standard deviations of daily returns) for 1960-1985 to the monthly VXO series for 1986-2017 from the St. Louis Fed's FRED database. Our quarterly VXO series uses within-quarter averages of the monthly series.

**Table 4: Variables in the baseline quarterly model**

GDP (100* $\Delta \ln$ )	GDP
Consumption (100* $\Delta \ln$ )	CONS
Private Investment (100* $\Delta \ln$ )	INVES
Hours (100* $\Delta \ln$ )	HOURS
Compensation of employees (100* $\Delta \ln$ )	COMPE
GDP deflator (100* $\Delta \ln$ )	PRICE
Federal funds rate ( $\Delta$ )	FFR
JLN or VXO uncertainty	uncertainty

**Table 5: Variables in the monthly model**

All employees: total nonfarm (100* $\Delta \ln$ )	PAYEM
Industrial production index (100* $\Delta \ln$ )	IP
Weekly hours: goods-producing (100* $\Delta \ln$ )	HOURS
Real consumer spending (100* $\Delta \ln$ )	SPEND
Orders (index/100)	ORDER
Earnings (100* $\Delta \ln$ )	EARNI
PCE price index (100* $\Delta \ln$ )	PCEPI
Federal funds rate ( $\Delta$ )	FFR
S&P 500 ( $\Delta \ln$ )	S&P
JLN or VXO uncertainty	uncertainty

The second model is a monthly VAR that includes nine monthly indicators in addition to the uncertainty measure. We will refer to this model as the monthly VAR. The variables included in the model are reported in Table 5.

This specification of variables is very similar to those considered in JLN and Bloom (2009), and contains many of the same variables in the VAR of Caldara, et al. (2016).<sup>17</sup> We use four lags and estimate over the sample 1961m7 to 2016m11, for a total of  $T = 659$

<sup>17</sup>We obtained very similar results with a model augmented to include a credit spread.

observations. As with the quarterly VAR, all variables are demeaned prior to estimation to reduce the computational burden. We obtained the monthly macroeconomic data from the MD-FRED database developed in McCracken and Ng (2016) and made available on the website of the Federal Reserve Bank of St. Louis.

Although the model is estimated with data transformed as indicated in Table 4 and Table 5, for comparability to previous studies, the impulse responses are cumulated and transformed back to the units typical in the literature. Accordingly, the units of the reported impulse responses are percentage point changes (based on 100 times log levels for variables in logs or rates for variables not in log terms). The fact that the model is estimated using some variables differenced for stationarity (e.g., GDP, consumption, and investment) implies that, for some of these variables, the long-run effects of transitory shocks do not die out.

## 5.2 Macroeconomic uncertainty shocks

Figure 7 shows the posterior distributions of the standard effect coefficients  $\phi$  and the feedback coefficients  $\psi$  under both the quarterly VAR (upper panels) and the monthly VAR (lower panels).

Focusing first on the standard effect coefficients  $\phi$ , which are on the left-hand side panels of Figure 7, they appear to be largely in line with previous findings about the effects of uncertainty on macroeconomic variables. In particular uncertainty has a large depressive effect on investment, output, consumption, hours, employment, industrial production, consumer spending, and earnings. A shock to uncertainty also leads to a loosening of the FFR, and an increase in inflation as measured by wages, the GDP deflator, and the PCE price index. These results confirm those of several other studies such as Baker, Bloom, and Davis (2016), Bloom (2009), Gilchrist, Sim, and Zakrajsek (2014), Jurado, Ludvigson, and Ng (2015), Jo and Sekkel (2017), and Carriero, Clark, and Marcellino (2017). They are also in line with the international evidence in Carriero, Clark, and Marcellino (2018a).

Turning our focus to the feedback coefficients  $\psi$ , which are on the right-hand side of Figure 7, it is striking that these coefficients do not appear to be statistically different from 0. This is especially true for the quarterly dataset, while some slight departure from 0 can be seen in the monthly dataset. The sign of the posterior means in this latter case is in line with what macroeconomic reasoning would expect, for example variables such as hours and industrial production tend to reduce uncertainty, whereas the FFR increases macroeconomic uncertainty. However, even in the monthly dataset, the overall picture is clearly one in which the contemporaneous effect of macroeconomic variables on uncertainty is feeble, if not entirely absent. It is also worth mentioning that these results are somewhat different from those reported in Figure 2. We attribute this difference to the fact that the

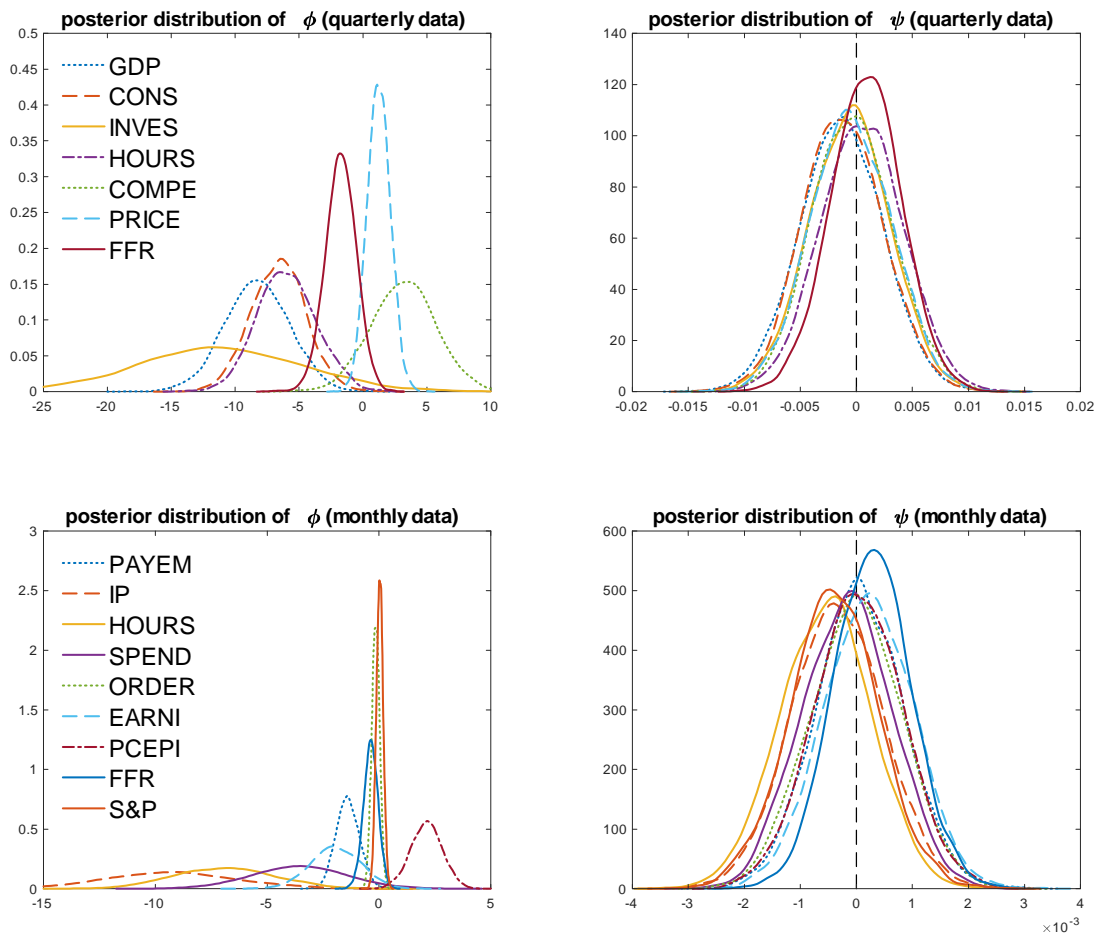


Figure 7: Posterior distribution of the  $\phi$  and  $\psi$  parameters. VARs with macro (JLN) uncertainty. Quarterly VAR in the upper panels, monthly VAR in the lower panels.

simple bivariate model omits several relevant variables, which leads to distortions in the estimated effects of uncertainty on output.

We now consider the consequences that shutting down the feedback coefficients  $\psi$  (which capture the immediate response of uncertainty to economic conditions) has on the coefficients  $\phi$  (which capture the immediate response of economic conditions to uncertainty) and on the impulse responses. This amounts to ordering uncertainty first in a VAR identified through a recursive Cholesky scheme. In light of both the results depicted in Figure 7 for the coefficients  $\psi$  and the results we obtained with the MC design in which  $\psi = 0$  in the DGP, we expect the distortion arising from shutting down the feedback effect to be small.

Figure 8 shows the time series path of the (posterior median of the) impulse responses to a macroeconomic uncertainty shock. Graphs in the first two rows provide results for the quarterly dataset, while graphs in the last two rows provide results for the monthly dataset.



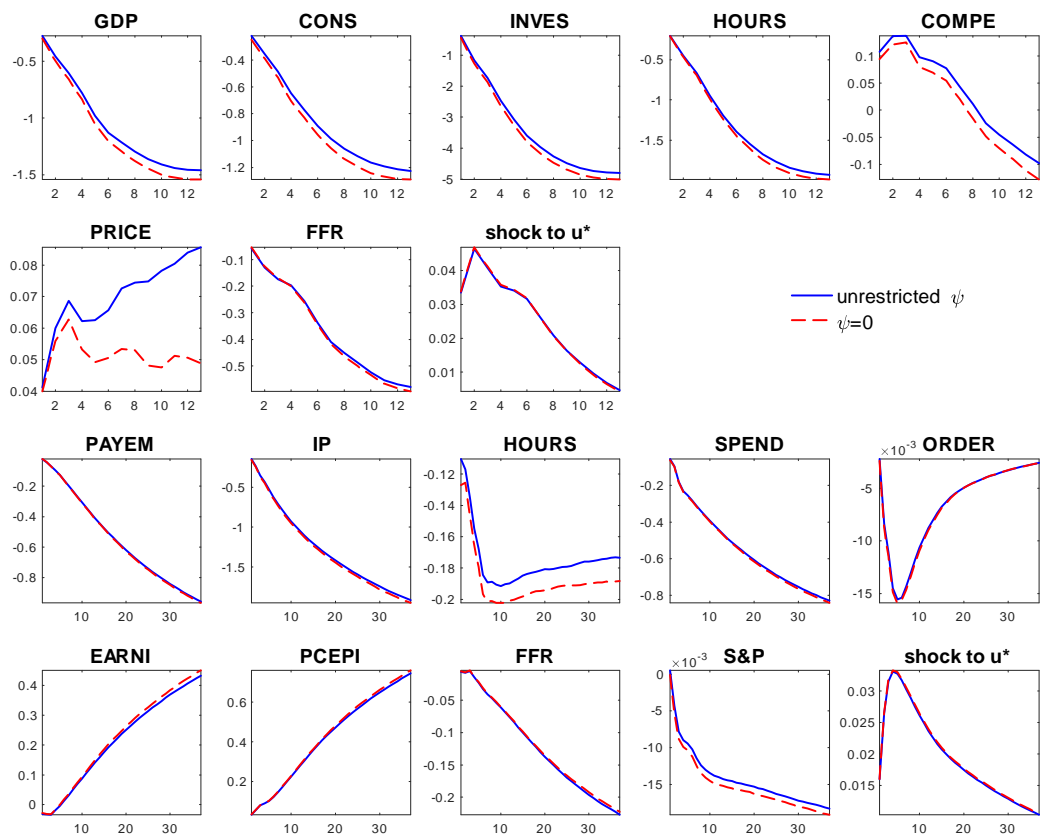


Figure 8: Impulse responses to a macro uncertainty shock with  $\psi = 0$  and  $\psi \neq 0$ . Rows 1 and 2: quarterly dataset. Rows 3 and 4: monthly dataset

In the figure, the unrestricted model is denoted by the solid blue lines, while the model with the feedback effects restricted to zero ( $\psi = 0$ ) is denoted by red dashed lines. It turns out that the differences between the two models are very small. An exception seems to be the path of quarterly prices, but it is important to note that this effect is estimated very imprecisely in both models, and that the resulting error bands around these responses (not shown for chart readability) are so wide that any difference between the posterior means is largely insignificant.

The fact that the differences in Figure 8 are barely noticeable, especially for the monthly dataset, might be due to a scaling effect, since the charts plot the time series evolution of the median, or might conceal differences in higher moments, rather than the posterior median. In order to check that this is not the case, Figure 14 and Figure 15 (in the Figure Appendix) display the entire posterior distribution of the impulse responses at some selected horizons. These figures show that setting  $\psi = 0$  has only a slight effect on impact and in the very short run. After that, the differences between the two models quickly die out, and the

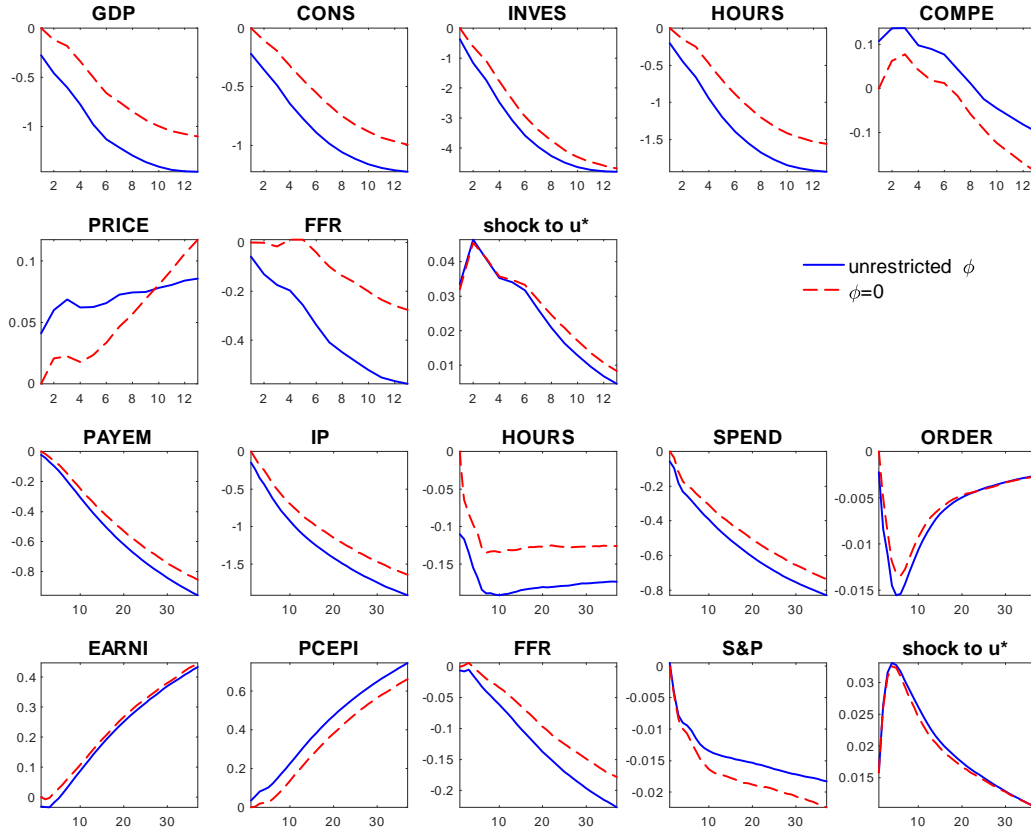


Figure 9: Impulse responses to a macro uncertainty shock with  $\phi = 0$  and  $\phi \neq 0$ . Rows 1 and 2: quarterly dataset. Rows 3 and 4: monthly dataset

distributions of the impulse responses become virtually identical.

It is interesting to also consider the case of shutting down the standard uncertainty effect (the contemporaneous effect of uncertainty on economic conditions), i.e., to set  $\phi = 0$ . This amounts to ordering uncertainty last in a VAR identified through a recursive Cholesky scheme. Since — as seen in Figure 7 — the coefficients  $\phi$  are broadly different from zero, and considering also the results we obtained with the MC design in which the researcher erroneously imposes  $\phi = 0$ , we expect the effect from shutting down this channel to be large.

Figure 9 shows the time series path of the (posterior median of the) impulse responses to a macroeconomic uncertainty shock, for the quarterly and monthly datasets, while Figure 16 and Figure 17 (in the Figure Appendix) display the entire posterior distribution of the impulse responses at some selected horizons. Clearly, shutting down the standard channel produces largely different impulse responses, which do not completely die out even at the 12-quarter- (or 36-month-) ahead horizons. These results, combined with the Monte Carlo evidence we discussed above (in particular, the design in which the researcher erroneously

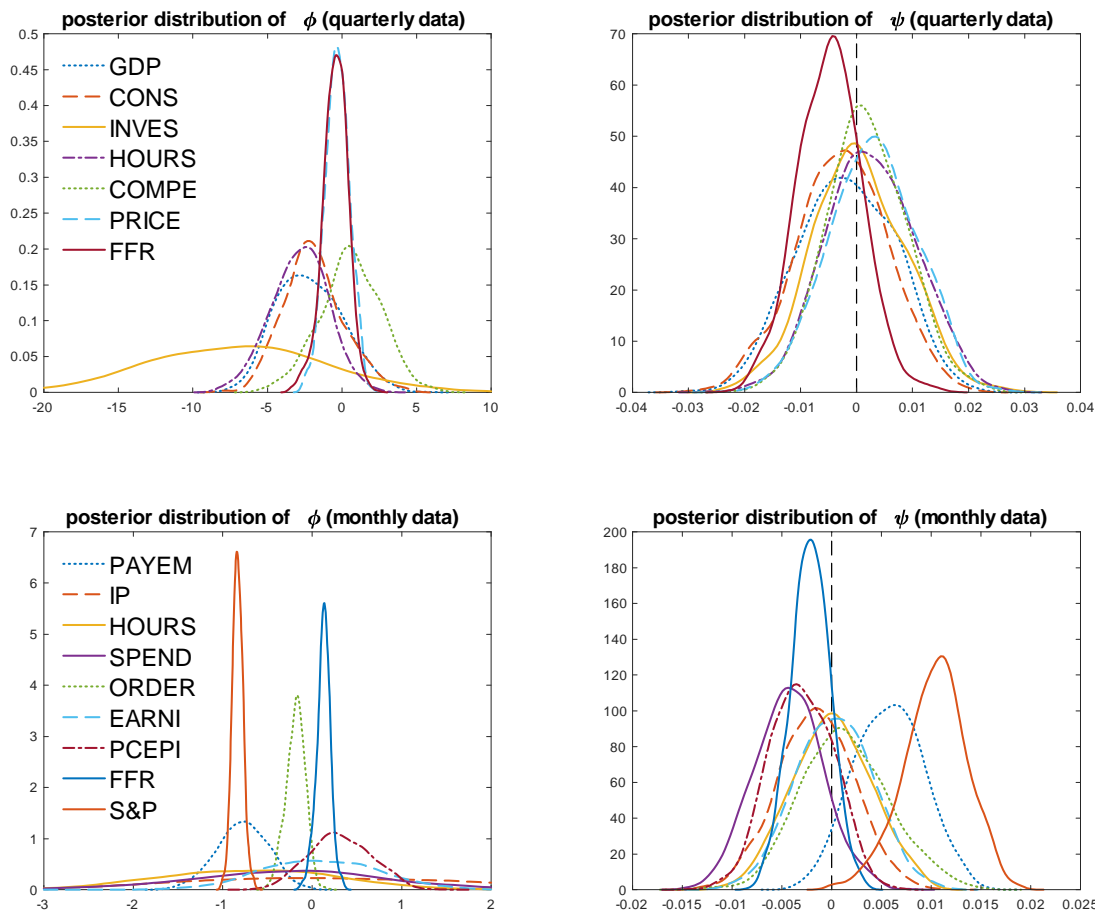


Figure 10: Posterior distribution of the  $\phi$  and  $\psi$  parameters. VARs with financial (VXO) uncertainty. Quarterly VAR in the upper panels, monthly VAR in the lower panels.

imposes  $\phi = 0$ ), imply that setting  $\phi = 0$  — or equivalently ordering macroeconomic uncertainty last in a recursive VAR — would very likely lead to distorted estimation of the effects of macro uncertainty shocks on macroeconomic variables, and a confusion between its contemporaneous and lagged effects.

### 5.3 Financial uncertainty shocks

We now focus on the effects of financial uncertainty shocks. Figure 10 shows the posterior distributions of the standard effect coefficients  $\phi$  (contemporaneous response of economic activity to uncertainty) and the feedback coefficients  $\psi$  (contemporaneous response of uncertainty to economic activity) under both the quarterly VAR (upper panels) and the monthly VAR (lower panels).

Focusing first on the standard effect coefficients  $\phi$ , which are on the left-hand side panels

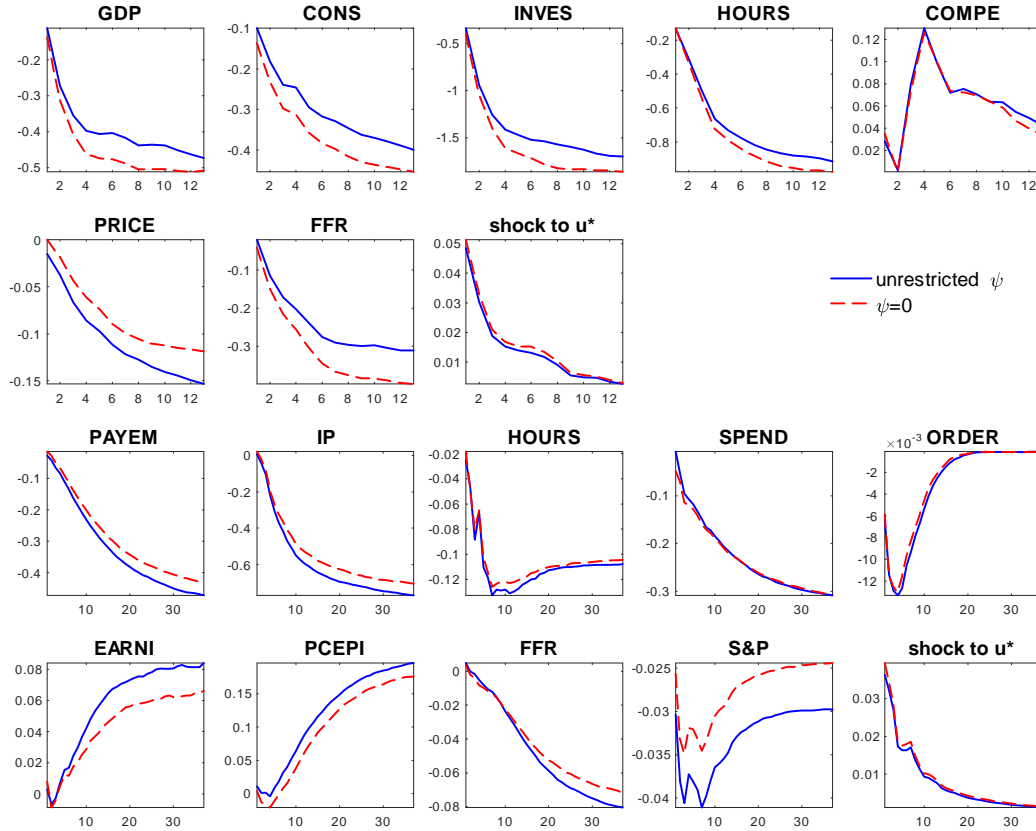


Figure 11: Impulse responses to a financial uncertainty shock with  $\psi = 0$  and  $\psi \neq 0$ . Rows 1 and 2: quarterly dataset. Rows 3 and 4: monthly dataset

of Figure 10, they appear to be largely in line with previous findings about the effects of financial uncertainty on macroeconomic variables. In particular, financial uncertainty has a large depressive effect on investment, output, consumption, hours, employment, and orders. Differently from what happened for macroeconomic uncertainty shocks (see Figure 7), financial uncertainty shocks do not seem to have a significant effect on the FFR, nor on prices as measured by wages, the GDP deflator, and the PCE price index. Instead, financial uncertainty shocks have a strong negative effect on the S&P500 index, while macroeconomic uncertainty shocks do not.

Turning to the feedback effect coefficients  $\psi$ , it is interesting to note that in the case of financial uncertainty there is more evidence that these coefficients are nonzero, i.e., that financial uncertainty might be endogenous. This pattern is particularly evident in the monthly dataset, with variables such as consumer spending, inflation, industrial production, and the FFR all featuring negative feedback coefficients, which shows that an increase in these indicators leads to a reduction in financial uncertainty. Some other variables show significantly

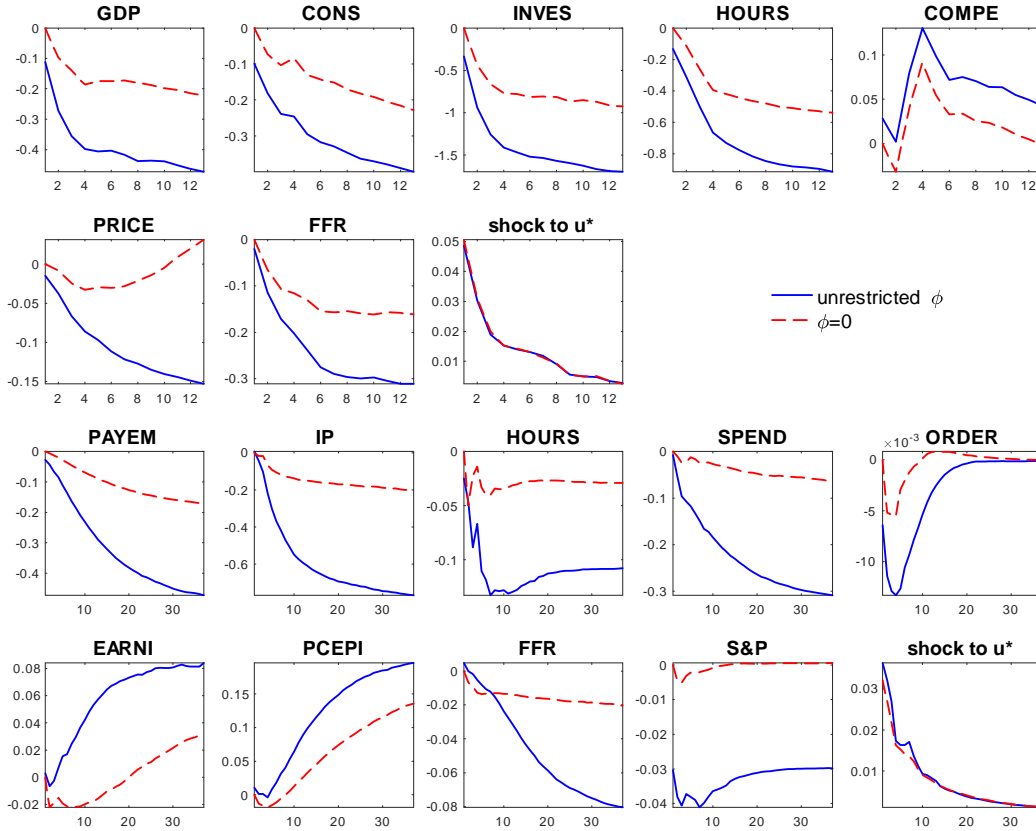


Figure 12: Impulse responses to a financial uncertainty shock with  $\phi = 0$  and  $\phi \neq 0$ . Rows 1 and 2: quarterly dataset. Rows 3 and 4: monthly dataset

positive  $\psi$  coefficients; in particular, increases in employment and the S&P index seem to increase uncertainty. The latter effect could be related to a risk-return relationship, but the former is somewhat less clear, perhaps linked to worries about a possible overheating of the economy and a monetary policy response. It is worth noting that the effect of the S&P500 on financial uncertainty is opposite to that on macro uncertainty. Also, nearly all of the probability mass of the posterior distribution of the parameter associated with the S&P500 is on positive values, which clearly suggests endogeneity of financial uncertainty, in contrast with the findings of LMN, who find less endogeneity in financial uncertainty with respect to macro uncertainty.<sup>18</sup>

Since for financial uncertainty we do find some evidence of endogeneity (i.e.,  $\psi \neq 0$ ) in the monthly dataset, we do expect (also in light of the Monte Carlo exercise) to find that imposing  $\psi = 0$  (i.e., ordering uncertainty first in a recursive VAR) would cause some dis-

<sup>18</sup>We have also added the S&P500 to the quarterly VAR model with VXO uncertainty. The posterior distribution of the  $\psi$  parameter associated with the S&P500 in this case is centered around zero, and there are virtually no differences in the other posterior densities.

tortions in the estimated coefficients  $\phi$  (the contemporaneous response of economic activity to uncertainty) and therefore in the impulse responses.

Figure 11 shows the time series path of the (posterior median of the) impulse responses to a financial uncertainty shock. As before, the two top rows of charts provide results for the quarterly dataset, while the two bottom rows provide results for the monthly dataset. In the figure, the unrestricted model is denoted by the solid blue lines, while the model with the feedback effects restricted to zero ( $\psi = 0$ ) is denoted by red dashed lines. As is clear from the figure, there are indeed some differences between the two models, particularly for those variables for which the coefficients  $\psi$  are far from zero, such as the FFR and the S&P index. Figure 18 and Figure 19 (in the Figure Appendix) report the entire posterior distribution of the impulse responses at some selected horizons for, respectively, quarterly and monthly data. With monthly data, shutting down the feedback effect by setting  $\psi = 0$  leads to a noticeable difference in the posterior distribution of the impulse responses, a difference that for some variables (employees and S&P500) lasts up to 12 periods (i.e., one year). These results indicate that financial uncertainty can at least in part arise as an endogenous response to some macroeconomic conditions, and that overlooking this channel would lead to a distorted estimate of the effects of financial uncertainty shocks on the economy.

Finally, we have repeated the exercise of shutting down the standard channel of transmission, i.e. setting the  $\phi$  coefficients to zero. This amounts to ordering financial uncertainty last in a VAR identified through a recursive Cholesky scheme. Since — as seen in Figure 10 — the coefficients  $\phi$  are broadly different from zero, we find that shutting down this channel has a large distortionary effect on the impulse responses, which does not completely die out even at the 12-quarter- (or 36-month-) ahead horizons. Therefore, just as happened with macroeconomic uncertainty, setting  $\phi = 0$  — or equivalently ordering financial uncertainty last in a recursive VAR — would very likely lead to a distorted estimate of the effects of financial uncertainty shocks on macroeconomic variables, and a confusion between its contemporaneous and lagged effects. This is indeed the case, as shown in Figure 12 above, and Figure 20 and Figure 21 in the Figure Appendix.

## 5.4 Summary

Our empirical results point to the conclusion that there is only mild evidence for the endogeneity of uncertainty, and this evidence is limited to financial uncertainty and, mainly, to the monthly dataset. When looking at macro uncertainty, we found strong evidence that the feedback coefficients  $\psi$  are likely close to zero, which means that imposing exogenous macroeconomic uncertainty does not do much harm. We found that some  $\psi$  coefficients are nonzero in the case of financial uncertainty, which points toward the conclusion that

financial uncertainty seems endogenous to some extent.

Our modeling approach does not put any restrictions on either  $\psi$  or  $\phi$ . Still, if a researcher wanted to use a recursive VAR, our results provide two important suggestions for identification. First, ordering macroeconomic uncertainty first is likely to be harmless, not necessarily so for financial uncertainty. Second, ordering either type of uncertainty last is likely to produce misleading results. These findings imply that, to reliably assess financial uncertainty and its macroeconomic effects, it is necessary to depart from a simple recursive ordering and use a more sophisticated approach to identification, such as the one we develop.

## 6 Conclusions

Uncertainty is a key variable to understanding economic dynamics, rather overlooked in the academic literature but attracting growing interest recently, partly following the Great Recession. Several theoretical and empirical papers are by now available on the effects of uncertainty on key economic variables. A general finding from the empirical studies is that uncertainty leads to a deterioration in economic conditions. However, this outcome could be at least partly due to an endogeneity problem. If economic conditions have a contemporaneous effect on uncertainty, ruling it out a priori could result in overestimation of the effects of uncertainty.

In this paper we have developed an econometric model where current and past values of uncertainty affect the current levels of economic variables, and uncertainty is in turn affected by them also contemporaneously. We achieve identification by means of a novel procedure that relies on a particular heteroskedasticity structure, which allows the time-varying conditional variances of the variables to be driven by an uncertainty measure plus an idiosyncratic component. We provide the relevant conditional posteriors for the states and coefficients of the model, which can be used to estimate the model using a Gibbs sampler.

Our results show that while macroeconomic uncertainty can be broadly considered exogenous, financial uncertainty can at least in part arise as an endogenous response to some macroeconomic developments, and that overlooking this channel would lead to a distorted estimate of the effects of financial uncertainty shocks on the economy.

## 7 Appendices

### 7.1 Details on identification

Starting from the model in (1) and (2), and following the notation in, e.g., Granziera, Moon, and Schorfheide (2017) define  $A^{-1}\Lambda_t^{0.5} = \Sigma_{tr,t}$ , which is a lower triangular Cholesky factor of  $\Sigma_t = A^{-1}\Lambda_t A^{-1'}$ . We also remove the intercepts, since they are not needed to discuss identification. The model becomes:

$$y_t = \Pi_y(L)y_{t-1} + \Pi_m(L)\ln m_{t-1} + \phi \ln m_t + \Sigma_{tr,t}\epsilon_t^* \quad (39)$$

$$\ln m_t = \delta_y(L)y_{t-1} + \delta_m(L)\ln m_{t-1} + \psi\epsilon_t^* + \tilde{u}_t. \quad (40)$$

Solving (39) for  $\epsilon_t^* = \Sigma_{tr,t}^{-1}(y_t - \Pi_y(L)y_{t-1} - \Pi_m(L)\ln m_{t-1} - \phi \ln m_t)$  and feeding it into (40) gives:

$$\begin{aligned} y_t &= \Pi_y(L)y_{t-1} + \Pi_m(L)\ln m_{t-1} + \phi \ln m_t + \Sigma_{tr,t}\epsilon_t^* \\ \ln m_t &= \delta_y(L)y_{t-1} + \delta_m(L)\ln m_{t-1} + \psi\Sigma_{tr,t}^{-1}(y_t - \Pi_y(L)y_{t-1} - \Pi_m(L)\ln m_{t-1} - \phi \ln m_t) + \tilde{u}_t, \end{aligned}$$

or,

$$\begin{aligned} \begin{bmatrix} I_n & -\phi \\ -\psi\Sigma_{tr,t}^{-1} & 1 + \psi\Sigma_{tr,t}^{-1}\phi \end{bmatrix} \begin{pmatrix} y_t \\ \ln m_t \end{pmatrix} &= \begin{bmatrix} \Pi_y & \Pi_m \\ \delta_y - \psi\Sigma_{tr,t}^{-1}\Pi_y & \delta_m - \psi\Sigma_{tr,t}^{-1}\Pi_m \end{bmatrix} \begin{pmatrix} y_{t-1} \\ \ln m_{t-1} \end{pmatrix} \\ &+ \begin{bmatrix} \Sigma_{tr,t} & 0 \\ 0 & 1 \end{bmatrix} \begin{pmatrix} \epsilon_t^* \\ \tilde{u}_t \end{pmatrix}, \end{aligned} \quad (41)$$

which represents the structural form.

The inverse of the matrix appearing in the left-hand side of (41) can be obtained by inverting the partitioned matrix:

$$\begin{aligned} \begin{bmatrix} I_n & -\phi \\ -\psi\Sigma_{tr,t}^{-1} & \kappa^{-1} \end{bmatrix}^{-1} &= \begin{bmatrix} (I_n - \phi\kappa\psi\Sigma_{tr,t}^{-1})^{-1} & (I_n - \phi\kappa\psi\Sigma_{tr,t}^{-1})^{-1}\phi\kappa \\ (\kappa^{-1} - \psi\Sigma_{tr,t}^{-1}I_n\phi)^{-1}\psi\Sigma_{tr,t}^{-1}I_n & (\kappa^{-1} - \psi\Sigma_{tr,t}^{-1}I_n\phi)^{-1} \end{bmatrix} \\ &= \begin{bmatrix} B & B\phi\kappa \\ \psi\Sigma_{tr,t}^{-1} & 1 \end{bmatrix}. \end{aligned} \quad (42)$$

where we defined

$$B_{n \times n} = (I_n - \phi\kappa\psi\Sigma_{tr,t}^{-1})^{-1}, \quad (43)$$

$$\kappa_{1 \times 1} = (1 + \psi\Sigma_{tr,t}^{-1}\phi)^{-1}. \quad (44)$$



The reduced form of the structural VAR in (41) can be obtained by pre-multiplying (41) by the inverse matrix in (42):

$$\begin{pmatrix} y_t \\ \ln m_t \end{pmatrix} = \begin{bmatrix} C_{11} & C_{21} \\ C_{12} & C_{22} \end{bmatrix} \begin{pmatrix} y_{t-1} \\ \ln m_{t-1} \end{pmatrix} + \begin{pmatrix} \epsilon_t \\ u_t \end{pmatrix}; \text{Var} \begin{pmatrix} \epsilon_t \\ u_t \end{pmatrix} = \begin{bmatrix} \Sigma_{11t} & \Sigma_{12t} \\ \Sigma_{12t} & \Sigma_{22t} \end{bmatrix} \quad (45)$$

with:

$$\begin{aligned} \begin{bmatrix} C_{11} & C_{21} \\ C_{12} & C_{22} \end{bmatrix} &= \begin{bmatrix} B & B\phi\kappa \\ \psi\Sigma_{tr,t}^{-1} & 1 \end{bmatrix} \begin{bmatrix} \Pi_y & \Pi_m \\ \delta_y - \psi\Sigma_{tr,t}^{-1}\Pi_y & \delta_m - \psi\Sigma_{tr,t}^{-1}\Pi_m \end{bmatrix} \\ &= \begin{bmatrix} B\Pi_y + B\kappa\phi\delta_y - B\kappa\phi\psi\Sigma_{tr,t}^{-1}\Pi_y & B\Pi_m + B\kappa\phi\delta_m - B\kappa\phi\psi\Sigma_{tr,t}^{-1}\Pi_m \\ \delta_y & \delta_m \end{bmatrix}, \\ \begin{bmatrix} \Sigma_{11t} & \Sigma_{12t} \\ \Sigma_{12t} & \Sigma_{22t} \end{bmatrix} &= \begin{bmatrix} B & B\phi\kappa \\ \psi\Sigma_{tr,t}^{-1} & 1 \end{bmatrix} \begin{bmatrix} \Sigma_{tr,t}\Sigma'_{tr,t} & 0 \\ 0 & \sigma_u^2 \end{bmatrix} \begin{bmatrix} B' & \Sigma_{tr,t}^{-1}\psi' \\ \kappa\phi'B' & 1 \end{bmatrix} \\ &= \begin{bmatrix} B\Sigma_{tr,t}B' + \kappa^2\sigma_u^2B\phi\phi'B' & B\Sigma_{tr,t}\psi' + \kappa\sigma_u^2B\phi \\ \psi'\Sigma'_{tr,t}B' + \kappa\sigma_u^2\phi'B' & \sigma_u^2 + \psi\psi' \end{bmatrix}. \end{aligned}$$

We can simplify some of the elements of the matrices above as follows:

$$\begin{aligned} C_{11} - \kappa B\phi\delta_y &= B(I - \kappa\phi\psi\Sigma_{tr,t}^{-1})\Pi_y = \Pi_y, \\ C_{21} - \kappa B\phi\delta_m &= B(I - \kappa\phi\psi\Sigma_{tr,t}^{-1})\Pi_m = \Pi_m \end{aligned}$$

where we used (43). Hence, it is:

$$\begin{aligned} C_{11} &= \Pi_y + \kappa B\phi\delta_y, \\ C_{21} &= \Pi_m + \kappa B\phi\delta_m, \\ C_{12} &= \delta_y, \\ C_{22} &= \delta_m, \\ \Sigma_{11t} &= B\Sigma_{tr,t}\Sigma'_{tr,t}B' + \kappa^2\sigma_u^2B\phi\phi'B', \\ \Sigma_{12t} &= B\Sigma_{tr,t}\psi' + \kappa\sigma_u^2B\phi, \\ \Sigma_{22} &= \sigma_u^2 + \psi\psi'. \end{aligned}$$

The system above is the one reported in (20). To obtain the system for the bivariate case it is sufficient to set  $n = 1$  and  $\Sigma_{tr,t} = \sqrt{m_t h_t}$  (a scalar). This implies<sup>19</sup>  $\kappa B = 1$ , and straightforward algebra leads to the system in (17).

---

<sup>19</sup>Because  $B = (I_1 - \kappa\phi\psi\Sigma_{tr,t}^{-1})^{-1} = (1 - (1 + \phi\Sigma_{tr,t}^{-1}\psi)^{-1}\phi\psi\Sigma_{tr,t}^{-1})^{-1} = \left(\frac{1 + \phi\Sigma_{tr,t}^{-1}\psi - \phi\psi\Sigma_{tr,t}^{-1}}{1 + \phi\Sigma_{tr,t}^{-1}\psi}\right)^{-1} = 1 + \frac{\phi\psi}{\sqrt{m_t h_t}} = \kappa^{-1}$

## 7.2 Derivation of the joint density of data and states

The starting point is the computation of the joint density of the data and the states  $p(y_t, m_t, h_t|\theta)$ , which can be obtained via the change of variable theorem.

We start by re-writing the shocks as follows:

$$\epsilon_t^* = m_t^{-0.5} H_t^{-0.5} A(y_t - \Pi_0 - \Pi_y(L)y_{t-1} - \Pi_m(L) \ln m_{t-1} - \phi \ln m_t), \quad (46)$$

$$\tilde{u}_t = \ln m_t - \alpha - \delta_y(L)y_{t-1} - \delta_m(L) \ln m_{t-1} - \psi \epsilon_t^*, \quad (47)$$

$$\tilde{\eta}_{jt} = \ln h_{jt} - \alpha_j - \delta_j \ln h_{jt-1}, \quad j = 1, \dots, n, \quad (48)$$

with:

$$\mathbf{r}_t = \begin{bmatrix} \epsilon_t^* \\ \tilde{u}_t \\ \tilde{\eta}_t \end{bmatrix} \sim N \left( \begin{bmatrix} 0 \\ 0 \\ 0 \end{bmatrix}, \begin{bmatrix} I_n & 0 & 0 \\ 0 & \sigma_{\tilde{u}}^2 & 0 \\ 0 & 0 & \Sigma_{\tilde{\eta}} \end{bmatrix} \right) \quad (49)$$

where  $\tilde{\eta}_t = (\tilde{\eta}_{1t}, \dots, \tilde{\eta}_{nt})'$  and  $\Sigma_{\tilde{\eta}}$  is a diagonal matrix with elements  $\sigma_{\tilde{\eta}_j}^2$ ,  $j = 1, \dots, n$ .<sup>20</sup> The vector  $\mathbf{r}_t$  is therefore a vector of independent Gaussian (structural) shocks.

Furthermore, we define:

$$\begin{aligned} e_t &= H_t^{0.5} \epsilon_t^* \\ &= m_t^{-0.5} A(y_t - \Pi_0 - \Pi_y(L)y_{t-1} - \Pi_m(L) \ln m_{t-1} - \phi \ln m_t) \\ u_t &= \psi \epsilon_t^* + \tilde{u}_t \end{aligned} \quad (50)$$

Note that  $e_t$  is observable conditioning on  $m_t$  and  $y_t$  (plus the coefficients in  $\theta_1$ ), while  $u_t$  is observable conditioning on  $m_t$  and  $y_t$  and  $\epsilon_t^*$  (plus the coefficients in  $\theta_2$ ).

Using the shocks (46)-(48) and:

$$JN_t = \begin{bmatrix} \partial \epsilon_t^* / \partial y_t & \partial \epsilon_t^* / \partial m_t & \partial \epsilon_t^* / \partial h_t \\ \partial \tilde{u}_t / \partial y_t & \partial \tilde{u}_t / \partial m_t & \partial \tilde{u}_t / \partial h_t \\ \partial \tilde{\eta}_t / \partial y_t & \partial \tilde{\eta}_t / \partial m_t & \partial \tilde{\eta}_t / \partial h_t \end{bmatrix}.$$

we can use the change of variable theorem to get:

$$p(y_t, m_t, h_t|\theta) = |JN_t| \times p_G(\epsilon_t^*, \tilde{u}_t, \tilde{\eta}_t). \quad (51)$$

Since  $\partial \tilde{\eta}_t / \partial y_t = \partial \tilde{\eta}_t / \partial m_t = 0$  and  $\partial \tilde{\eta}_t / \partial h_t = H_t^{-1}$ , it is:

$$|JN_t| = |H_t^{-1}| \left| \begin{pmatrix} \partial \epsilon_t^* / \partial y_t & \partial \epsilon_t^* / \partial m_t \\ \partial \tilde{u}_t / \partial y_t & \partial \tilde{u}_t / \partial m_t \end{pmatrix} \right|,$$

<sup>20</sup>The assumption that the shocks to  $h_t$  are independent can be easily removed.

with

$$\partial\epsilon_t^*/\partial y_t = m_t^{-0.5} H_t^{-0.5} A, \quad (52)$$

$$\partial\tilde{u}_t/\partial y_t = -\psi\partial\epsilon_t^*/\partial y_t, \quad (53)$$

$$\partial\tilde{u}_t/\partial m_t = m_t^{-1} - \psi\partial\epsilon_t^*/\partial m_t. \quad (54)$$

Hence, the determinant is:

$$\begin{aligned} |JN_t| &= |H_t^{-1}||\partial\epsilon_t^*/\partial y_t| * |\partial\tilde{u}_t/\partial m_t - \partial\tilde{u}_t/\partial y_t * (\partial\epsilon_t^*/\partial y_t)^{-1} * \partial\epsilon_t^*/\partial m_t| = \\ &= |H_t^{-1}||\partial\epsilon_t^*/\partial y_t| * |\partial\tilde{u}_t/\partial m_t + \psi\partial\epsilon_t^*/\partial y_t * (\partial\epsilon_t^*/\partial y_t)^{-1} * \partial\epsilon_t^*/\partial m_t| = \\ &= |H_t^{-1}||\partial\epsilon_t^*/\partial y_t| * |m_t^{-1} - \psi\partial\epsilon_t^*/\partial m_t + \psi * \partial\epsilon_t^*/\partial m_t| = \\ &= |H_t^{-1}||\partial\epsilon_t^*/\partial y_t| * |m_t^{-1}| = m_t^{-0.5n} \prod_{j=1}^n h_{jt}^{-1.5} |A| * m_t^{-1} = \\ &= m_t^{-1-0.5n} \prod_{j=1}^n h_{jt}^{-1.5}. \end{aligned}$$

Therefore,

$$\begin{aligned} p(y_t, m_t, h_t|\theta) &= m_t^{-1-0.5n} \prod_{j=1}^n h_{jt}^{-1.5} \times p_G(\epsilon_t^*, \tilde{u}_t, \tilde{\eta}_t) \\ &= \underbrace{m_t^{-1-0.5n} \prod_{j=1}^n h_{jt}^{-1.5} p_G(\epsilon_t^*)}_{\text{eq. (1)}} \times \underbrace{p_G(\tilde{u}_t)}_{\text{eq. (2)}} \times \underbrace{p_G(\tilde{\eta}_t)}_{\text{eq. (4)}}, \end{aligned} \quad (55)$$

where it is clear which pieces are coming from equations (1)-(4).

### 7.3 Derivation of the conditional posterior of the states

In this subsection we derive the expression for the conditional posterior of the states in equation (26). To do so we consider the data density (55) for the generic volatility of variable  $j$  at time  $t$  (i.e.  $h_{jt}$ ) and recognize that i) since mutual independence of the shocks ensures that  $p_G(\epsilon_t^*) = \prod_{j=1}^n p_G(\epsilon_{jt}^*)$  and  $p_G(\tilde{\eta}_t) = \prod_{j=1}^n p_G(\tilde{\eta}_{jt})$ , all the terms not involving variable  $j$  can be subsumed in the integrating constant; ii) due to the Markov property featured by  $h_{jt}$ , all the terms involving time periods beyond  $t-1$  or  $t+1$  can be ignored.<sup>21</sup>

This gives:

$$p(h_{jt}|h_{jt-1}, h_{jt+1}, \theta, \mathbf{y}_{1:T}, \mathbf{m}_{1:T}, \mathbf{h}_{\neq j 1:T}) \propto h_{jt}^{-1.5} p_G(\epsilon_{jt}^*) \times p_G(\tilde{u}_t) \times p_G(\tilde{\eta}_{jt}) \quad (56)$$

$$= h_{jt}^{-1.5} \exp\left(\frac{-\epsilon_{jt}^{*2} - \epsilon_{jt+1}^{*2}}{2}\right) \quad (57)$$

$$\times \exp\left(\frac{-\tilde{u}_t^2 - \tilde{u}_{t+1}^2}{2\sigma_u^2}\right) \quad (58)$$

$$\times \exp\left(\frac{-\tilde{\eta}_{jt}^2 - \tilde{\eta}_{jt+1}^2}{2\sigma_{\tilde{\eta}}^2}\right), \quad (59)$$

---

<sup>21</sup>These initial derivation steps follow the approach of Jacquier, Polson, and Rossi (2004). However, as we stressed in Section 2, our model is more general than theirs.

where we also subsumed  $m_t^{-1-0.5n}$  and all of the terms  $h_{it}^{-1.5}$  with  $i \neq j$  in the integrating constant. Furthermore, the terms  $\epsilon_{jt+1}^{*2}$  and  $\tilde{u}_{t+1}^2$  are also redundant, while the term  $\exp\left(\frac{-\tilde{\eta}_{jt}^2 - \tilde{\eta}_{jt+1}^2}{2\sigma_{\tilde{\eta}}^2}\right)$  will be used in the usual way as a proposal kernel. The term  $\exp\left(\frac{-\tilde{u}_t^2}{2\sigma_{\tilde{u}}^2}\right)$  can be written as:

$$\exp\left(\frac{-\tilde{u}_t^2}{2\sigma_{\tilde{u}}^2}\right) = \exp\left(\frac{-(u_t - \psi\epsilon_t^*)^2}{2\sigma_{\tilde{u}}^2}\right) = \exp\left(\frac{-u_t^2 + 2u_t\psi\epsilon_t^* - \epsilon_t^{*\prime}\psi'\psi\epsilon_t^*}{2\sigma_{\tilde{u}}^2}\right),$$

and, as  $u_t$  is observed under the conditioning set, this becomes

$$\exp\left(\frac{-\tilde{u}_t^2}{2\sigma_{\tilde{u}}^2}\right) \propto \exp\left(\frac{2u_t\psi\epsilon_t^* - \epsilon_t^{*\prime}\psi'\psi\epsilon_t^*}{2\sigma_{\tilde{u}}^2}\right), \quad (60)$$

where  $\exp(u_t\psi\epsilon_t^* = u_t\psi_1\epsilon_{1t}^* + u_t\psi_2\epsilon_{2t}^* + \dots + u_t\psi_n\epsilon_{nt}^*) \propto \exp(u_t\psi_j\epsilon_{jt}^*)$ . Also, since:

$$\begin{aligned} & (\psi_1\epsilon_{1t}^* + \psi_2\epsilon_{2t}^* + \dots + \psi_n\epsilon_{nt}^*) \times (\psi_1\epsilon_{1t}^* + \psi_2\epsilon_{2t}^* + \dots + \psi_n\epsilon_{nt}^*) \\ = & \psi_1\epsilon_{1t}^* \times (\psi_1\epsilon_{1t}^* + \psi_2\epsilon_{2t}^* + \dots + \psi_n\epsilon_{nt}^*) \\ & + \psi_2\epsilon_{2t}^* \times (\psi_1\epsilon_{1t}^* + \psi_2\epsilon_{2t}^* + \dots + \psi_n\epsilon_{nt}^*) \\ & \dots \\ & + \psi_j\epsilon_{jt}^* \times (\psi_1\epsilon_{1t}^* + \psi_2\epsilon_{2t}^* + \dots + \psi_n\epsilon_{nt}^*) \\ & \dots \\ & + \psi_n\epsilon_{nt}^* \times (\psi_1\epsilon_{1t}^* + \psi_2\epsilon_{2t}^* + \dots + \psi_n\epsilon_{nt}^*), \end{aligned}$$

we have that for a given equation  $j$  and conditioning on the remaining equations  $\exp(\epsilon_t^{*\prime}\psi'\psi\epsilon_t^*) \propto \exp(\epsilon_{jt}^{*2}\psi_j^2 + 2\psi_j\epsilon_{jt}^*(\psi_1\epsilon_{1t}^* + \dots + \psi_{j-1}\epsilon_{j-1t}^* + \psi_{j+1}\epsilon_{j+1t}^* + \dots + \psi_n\epsilon_{nt}^*))$ . This leads to:

$$\exp\left(\frac{-\tilde{u}_t^2}{2\sigma_{\tilde{u}}^2}\right) \propto \exp\left(\frac{2u_t\psi_j\epsilon_{jt}^* - (\epsilon_{jt}^{*2}\psi_j^2 + 2\epsilon_{jt}^*\psi_j\psi_{\neq j}\epsilon_{\neq jt}^*)}{2\sigma_{\tilde{u}}^2}\right) \quad (61)$$

$$= \exp\left(-\frac{e_{jt}^2\psi_j^2}{2\sigma_{\tilde{u}}^2 h_{jt}} + \frac{e_{jt}\psi_j}{\sqrt{h_{jt}\sigma_{\tilde{u}}^2}}[u_t - \psi_{\neq j}\epsilon_{\neq jt}^*]\right), \quad (62)$$

where  $\psi_j$  is the  $j$ -th element of the vector  $\psi$  and  $\psi_{\neq j}$  is the vector obtained by removing the element  $\psi_j$  from  $\psi$ . Using  $\epsilon_{jt}^* = h_{jt}^{-0.5}e_{jt}$  gives:

$$\exp\left(-\frac{\epsilon_{jt}^{*2}}{2} - \frac{\tilde{u}_t^2}{2\sigma_{\tilde{u}}^2}\right) \propto \exp\left(-\frac{e_{jt}^2}{2h_{jt}} - \frac{e_{jt}^2\psi_j^2}{2\sigma_{\tilde{u}}^2 h_{jt}} + \frac{e_{jt}\psi_j}{\sqrt{h_{jt}\sigma_{\tilde{u}}^2}}[u_t - \psi_{\neq j}\epsilon_{\neq jt}^*]\right), \quad (63)$$

and:

$$\begin{aligned} & p(h_{jt}|h_{jt-1}, h_{jt+1}, \theta, \mathbf{y}_{1:T}, \mathbf{m}_{1:T}, \mathbf{h}_{\neq j1:T}) \\ \propto & h_{jt}^{-0.5} \exp\left(-\frac{e_{jt}^2}{2h_{jt}} \left[1 + \frac{\psi_j^2}{\sigma_{\tilde{u}}^2}\right] + \frac{e_{jt}}{\sqrt{h_{jt}}}\frac{\psi_j}{\sigma_{\tilde{u}}^2}[u_t - \psi_{\neq j}\epsilon_{\neq jt}^*]\right) \times h_{jt}^{-1} \exp\left(\frac{-\left(\ln h_{jt}^2 - \mu_{jt}\right)^2}{\sigma_{\tilde{\eta}}^2}\right), \end{aligned}$$

which is the conditional posterior of the states appearing in (26).

## 7.4 Mixing and convergence diagnostics for the multivariate model

In this section we evaluate the convergence and mixing properties of the MCMC sampler. Figure 13 reports the potential scale reduction factors and inefficiency factors for all of the coefficients in the model for the monthly dataset with macro uncertainty (results are very similar for all the other specifications). The results are organized in groups, so that results for the coefficients in the  $y_t$  equations ( $\theta_1$ ) are reported in the plots in the first column on the left-hand side, results for the coefficients in the uncertainty equation ( $\theta_2$ ) are reported in the plots in the central column, and results for the coefficients of the idiosyncratic volatilities processes ( $\theta_3$ ) are reported in the plots in the last column, on the right-hand side.

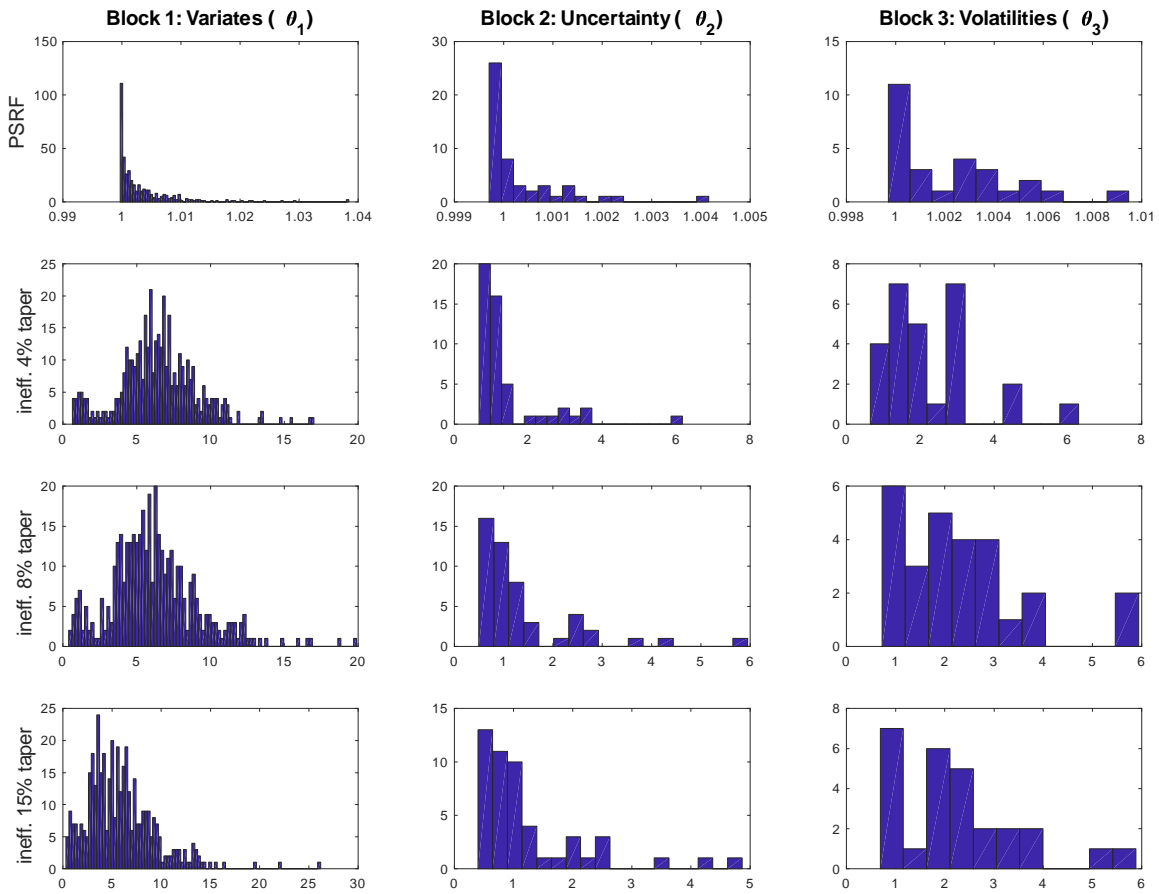


Figure 13: Potential scale reduction factors and inefficiency factors for the simulated draws of the model coefficients.

## References

- [1] Angelini, G., Bacchiocchi, E., Caggiano, G., Fanelli, L. (2017), Uncertainty across volatility regimes, Bank of Finland Research Discussion Paper N. 35/17
- [2] Arellano, C., Y. Bai, and P. Kehoe (2016), “Financial Frictions and Fluctuations in Volatility,” NBER Working Paper 22990. <https://doi.org/10.3386/w22990>
- [3] Bachmann, R., and G. Moscarini (2011), “Business Cycles and Endogenous Uncertainty,” Discussion paper, Society for Economic Dynamics.
- [4] Bachmann, R., S. Elstner, and E. Sims (2013), “Uncertainty and Economic Activity: Evidence from Business Survey Data,” *American Economic Journal: Macroeconomics* 5, 217-249. <https://doi.org/10.1257/mac.5.2.217>
- [5] Baker S., N. Bloom, and S. Davis (2016), “Measuring Economic Policy Uncertainty,” *Quarterly Journal of Economics* 131(4), 1593-1636. <https://doi.org/10.1093/qje/qjw024>
- [6] Basu S., and B. Bundick (2017), “Uncertainty Shocks in a Model of Effective Demand,” *Econometrica* 85(3), 937-958. <https://doi.org/10.3982/ECTA13960>
- [7] Bernanke, B. (1983), “Irreversibility, Uncertainty, and Cyclical Investment,” *Quarterly Journal of Economics* 98(1), 85-106. <https://doi.org/10.2307/1885568>
- [8] Bernanke, B., J. Boivin, and P. Elias (2005), “Measuring the Effects of Monetary Policy: A Factor-Augmented Vector Autoregressive (FAVAR) Approach,” *Quarterly Journal of Economics* 120, 387-422. <https://doi.org/10.1162/0033553053327452>
- [9] Bloom, N. (2009), “The Impact of Uncertainty Shocks,” *Econometrica* 77(3), 623-685. <https://doi.org/10.3982/ECTA6248>
- [10] Bloom, N. (2014), “Fluctuations in Uncertainty,” *Journal of Economic Perspectives* 28(2), 153-176. <https://doi.org/10.1257/jep.28.2.153>
- [11] Bloom N., M. Floetotto, M. Jaimovich, I. Saporta-Eksten, and S. Terry (2012), “Really Uncertain Business Cycles,” NBER Working Paper 18245. <https://doi.org/10.3386/w18245>
- [12] Bognanni, M. (2017), “A Class of Time-Varying Parameter Structural VARs for Inference under Exact or Partial Identification,” manuscript.

- [13] Caggiano, G., E. Castelnuovo, and N. Groshenny (2014), "Uncertainty Shocks and Unemployment Dynamics: An Analysis of Post-WWII US Recessions," *Journal of Monetary Economics* 67, 78-92. <https://doi.org/10.1016/j.jmoneco.2014.07.006>
- [14] Caldara, D., C. Fuentes-Albero, S. Gilchrist, and E. Zakrajsek (2016), "The Macroeconomic Impact of Financial and Uncertainty Shocks," *European Economic Review* 88, 185-207. <https://doi.org/10.1016/j.euroecorev.2016.02.020>
- [15] Campbell, J., M. Lettau, B. Malkiel, and Y. Xu (2001), "Have Individual Stocks Become More Volatile? An Empirical Exploration of Idiosyncratic Risk," *Journal of Finance* 56, 1-43. <https://doi.org/10.1111/0022-1082.00318>
- [16] Carriero, A., T. Clark, and M. Marcellino (2017), "Measuring Uncertainty and Its Impact on the Economy," *Review of Economics and Statistics*, forthcoming. [https://doi.org/10.1162/REST\\_a\\_00693](https://doi.org/10.1162/REST_a_00693)
- [17] Carriero, A., T. Clark, and M. Marcellino (2018a), "Assessing International Commonality in Macroeconomic Uncertainty and its Effects," Federal Reserve Bank of Cleveland Working Paper 18-03. <https://doi.org/10.26509/frbc-wp-201803>
- [18] Carriero, A., T. Clark, and M. Marcellino (2018b), "Large Bayesian Vector Autoregressions with Stochastic Volatility and Non-Conjugate Priors," manuscript.
- [19] Cesa-Bianchi, A., M. Pesaran, and A. Rebucci (2017), "Uncertainty and Economic Activity: Identification Through Cross-Country Correlations," manuscript.
- [20] Chan, J.C.C., and E. Eisenstat (2018), "Bayesian Model Comparison for Time-Varying Parameter VARs with Stochastic Volatility," *Journal of Applied Econometrics*, in press. <https://doi.org/10.1002/jae.2617>
- [21] Fajgelbaum, P., E. Schaal, and M. Taschereau-Dumouchel (2014), "Uncertainty Traps," NBER Working Paper 19973. <https://doi.org/10.3386/w19973>
- [22] Fernandez-Villaverde, J., P. Guerron-Quintana, J. Rubio-Ramirez, and M. Uribe (2011), "Risk Matters: The Real Effects of Volatility Shocks," *American Economic Review* 101(6), 2530-2561. <https://doi.org/10.1257/aer.101.6.2530>
- [23] Gilchrist S., J. Sim, and E. Zakrajsek (2014), "Uncertainty, Financial Frictions, and Investment Dynamics," NBER Working Paper 20038. <https://doi.org/10.3386/w20038>

- [24] Granziera, E., H. Moon, and F. Schorfheide (2017), "Inference for VARs Identified with Sign Restrictions," manuscript.
- [25] Hamilton, J.D. (1994), *Time Series Analysis*, Princeton, N.J.: Princeton University Press.
- [26] Jacquier, E., N. Polson, and P. Rossi (2004), "Bayesian Analysis of Stochastic Volatility Models with Fat-Tails and Correlated Errors," *Journal of Econometrics* 122, 185-212. <https://doi.org/10.1016/j.jeconom.2003.09.001>
- [27] Jo, S., and R. Sekkel (2017), "Macroeconomic Uncertainty Through the Lens of Professional Forecasters," Federal Reserve Bank of Dallas, Research Department Working Paper 1702. <https://doi.org/10.24149/wp1702>
- [28] Jurado, K., S. Ludvigson, and S. Ng (2015), "Measuring Uncertainty," *American Economic Review* 105, 1177-1216. <https://doi.org/10.1257/aer.20131193>
- [29] Justiniano, A., G. Primiceri, and A. Tambalotti (2011), "Investment Shocks and the Relative Price of Investment," *Review of Economic Dynamics* 14, 102-121. <https://doi.org/10.1016/j.red.2010.08.004>
- [30] Kilian, L., and H. Lütkepohl (2017), *Structural Vector Autoregressive Analysis*, Cambridge University Press. <https://doi.org/10.1017/9781108164818>
- [31] Lanne, M., and H. Lütkepohl (2008), "Identifying Monetary Policy Shocks via Changes in Volatility," *Journal of Money, Credit, and Banking* 40, 1131-1149. <https://doi.org/10.1111/j.1538-4616.2008.00151.x>
- [32] Lanne, M., H. Lütkepohl, and K. Maciejowska (2010), "Structural Vector Autoregressions with Markov Switching," *Journal of Economic Dynamics and Control* 34, 121-131. <https://doi.org/10.1016/j.jedc.2009.08.002>
- [33] Lanne, M., M. Meitz, and P. Saikkonen (2017), "Identification and Estimation of non-Gaussian Structural Vector Autoregressions," *Journal of Econometrics* 196, 288-304. <https://doi.org/10.1016/j.jeconom.2016.06.002>
- [34] Leduc S., and Z. Liu (2012), "Uncertainty Shocks Are Aggregate Demand Shocks," *Journal of Monetary Economics* 82, 20-35. <https://doi.org/10.1016/j.jmoneco.2016.07.002>
- [35] Lewis, D. (2017), "Identifying Shocks via Time-Varying Volatility," manuscript, Harvard University.



- [36] Ludvigson, S., S. Ma, and S. Ng (2018), “Uncertainty and Business Cycles: Exogenous Impulse or Endogenous Response?” manuscript.
- [37] Lütkepohl, H., and A. Netšunajev (2014), “Structural Vector Autoregressions with Smooth Transition in Variances: The Interaction between U.S. Monetary Policy and the Stock Market,” DIW Discussion Paper 1388. <https://doi.org/10.2139/ssrn.2456126>
- [38] McCracken, M., and S. Ng, (2016), “FRED-MD: A Monthly Database for Macroeconomic Research,” *Journal of Business and Economic Statistics* 34, 574-589. <https://doi.org/10.1080/07350015.2015.1086655>
- [39] McDonald, R., and D. Siegel (1986), “The Value of Waiting to Invest,” *Quarterly Journal of Economics* 101(4), 707-727. <https://doi.org/10.2307/1884175>
- [40] Normandin, M., and L. Phaneuf (2004), “Monetary Policy Shocks: Testing Identification Conditions Under Time-Varying Conditional Volatility,” *Journal of Monetary Economics* 51, 1217-1243. [https://doi.org/10.1016/S0304-3932\(04\)00069-8](https://doi.org/10.1016/S0304-3932(04)00069-8)
- Primiceri, G.E. (2005), “Time-Varying Structural Vector Autoregressions and Monetary Policy,” *Review of Economic Studies* 72, 821-852. DOI:10.1111/j.1467-937X.2005.00353.x
- [41] Rigobon, R. (2003), “Identification through Heteroskedasticity,” *Review of Economics and Statistics* 85, 777-792. <https://doi.org/10.1162/003465303772815727>
- [42] Rossi, B., and T. Sekhposyan (2015), “Macroeconomic Uncertainty Indices Based on Nowcast and Forecast Error Distributions,” *American Economic Review* 105, 650-655. <https://doi.org/10.1257/aer.p20151124>
- [43] Rubio-Ramirez, J.F., D.F. Waggoner, and T. Zha (2010), “Structural Vector Autoregressions: Theory of Identification and Algorithms for Inference,” *Review of Economic Studies* 77(2), 665-696. <https://doi.org/10.1111/j.1467-937X.2009.00578.x>
- [44] Sentana, E., G. Fiorentini (2011), “Identification, Estimation and Testing of Conditionally Heteroskedastic Factor Models,” *Journal of Econometrics* 102, 143-164. [https://doi.org/10.1016/S0304-4076\(01\)00051-3](https://doi.org/10.1016/S0304-4076(01)00051-3)
- [45] Shin, M., and M. Zhong (2018), “A New Approach to Identifying the Real Effects of Uncertainty Shocks,” manuscript.
- [46] Sims, C., and Zha, T., (1998), “Bayesian Methods for Dynamic Multivariate Models,” *International Economic Review* 39, 949-968. <https://doi.org/10.2307/2527347>

Smets, F., and R. Wouters (2007), "Shocks And Frictions In US Business Cycles: A Bayesian DSGE Approach," *American Economic Review* 97, 586-606. <https://doi.org/10.1257/aer.97.3.586>

## 8 Figure Appendix

This Appendix contains the simulated distributions of the impulse response functions at selected forecast horizons ( $h=0, 1, 4,$  and  $12$  quarters ahead for the quarterly model and  $h=0,3,12,36$  for the monthly model), for the following cases:

- Figure 14: Macro uncertainty shock, quarterly data, effect of imposing  $\psi = 0$
- Figure 15: Macro uncertainty shock, monthly data, effect of imposing  $\psi = 0$
- Figure 16: Macro uncertainty shock, quarterly data, effect of imposing  $\phi = 0$
- Figure 17: Macro uncertainty shock, monthly data, effect of imposing  $\phi = 0$
- Figure 18: Financial uncertainty shock, quarterly data, effect of imposing  $\psi = 0$
- Figure 19: Financial uncertainty shock, monthly data, effect of imposing  $\psi = 0$
- Figure 20: Financial uncertainty shock, quarterly data, effect of imposing  $\phi = 0$
- Figure 21: Financial uncertainty shock, monthly data, effect of imposing  $\phi = 0$

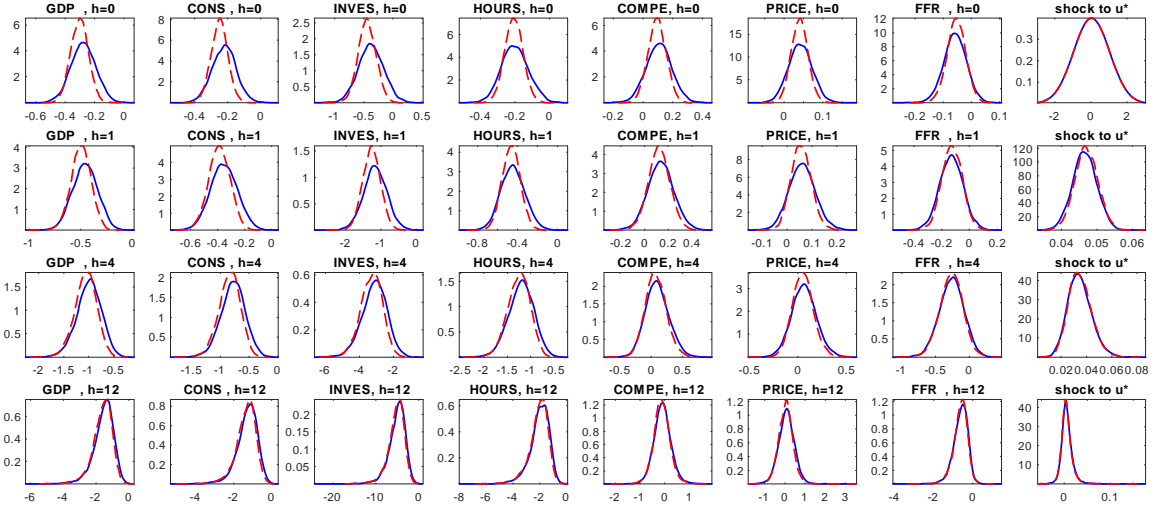


Figure 14: Macro uncertainty shock, quarterly data. Distribution of impulse responses at selected horizons. Blue solid line denotes the case  $\psi \neq 0$ , red dashed line denotes the case  $\psi = 0$ .

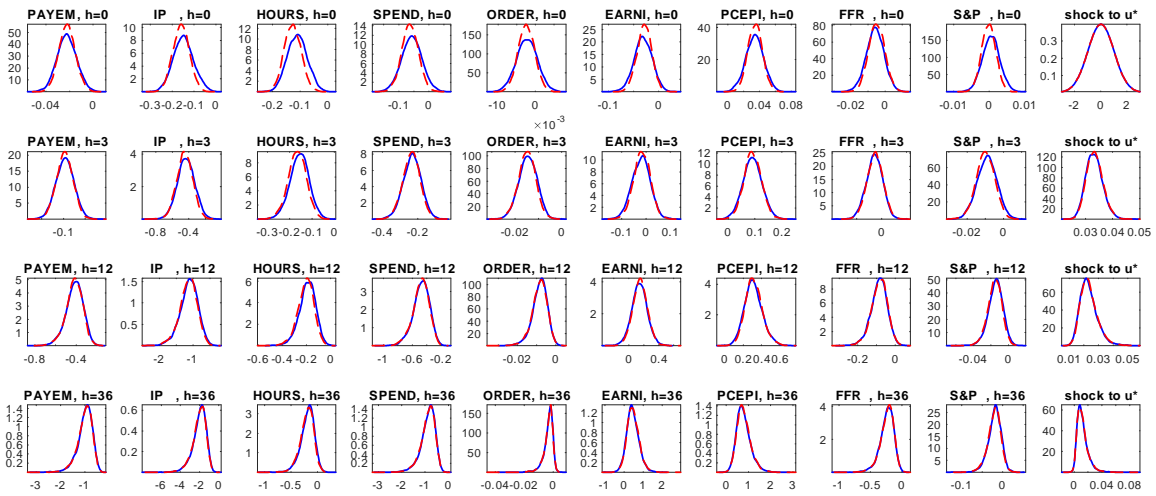


Figure 15: Macro uncertainty shock, monthly data. Distribution of impulse responses at selected horizons. Blue solid line denotes the case  $\psi \neq 0$ , red dashed line denotes the case  $\psi = 0$ .

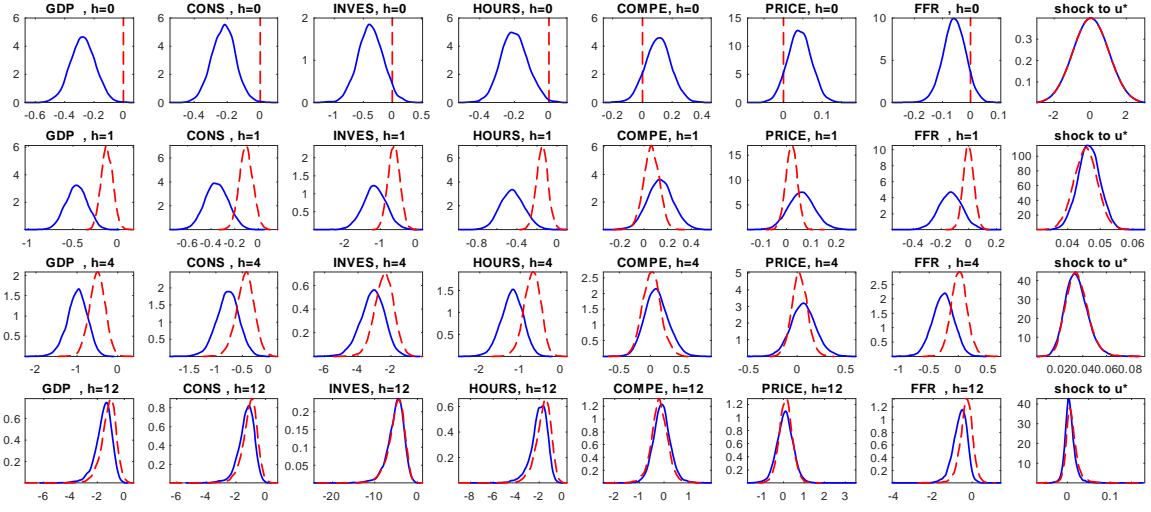


Figure 16: Macro uncertainty shock, quarterly data. Distribution of impulse responses at selected horizons. Blue solid line denotes the case  $\phi \neq 0$ , red dashed line denotes the case  $\phi = 0$ .

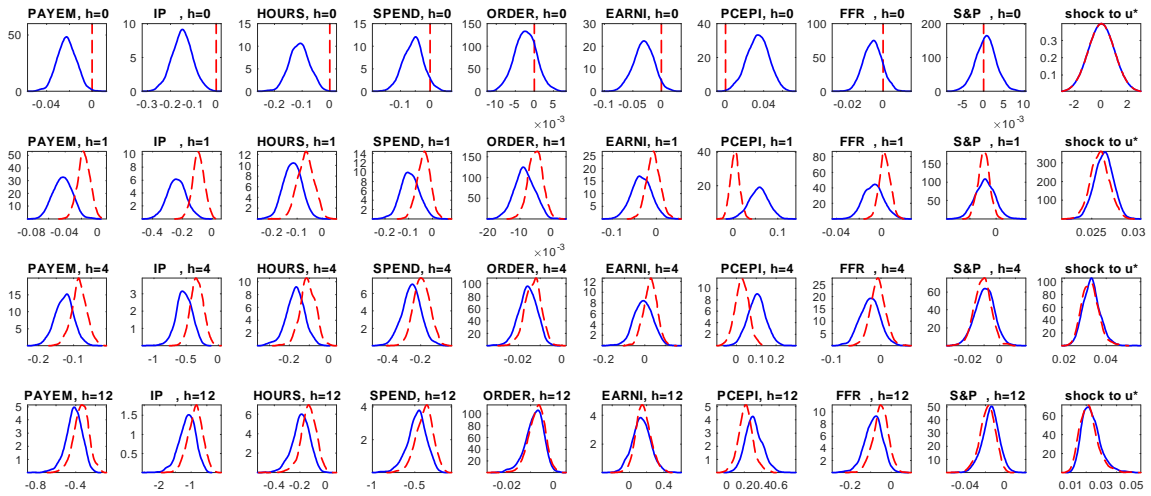


Figure 17: Macro uncertainty shock, monthly data. Distribution of impulse responses at selected horizons. Blue solid line denotes the case  $\phi \neq 0$ , red dashed line denotes the case  $\phi = 0$ .

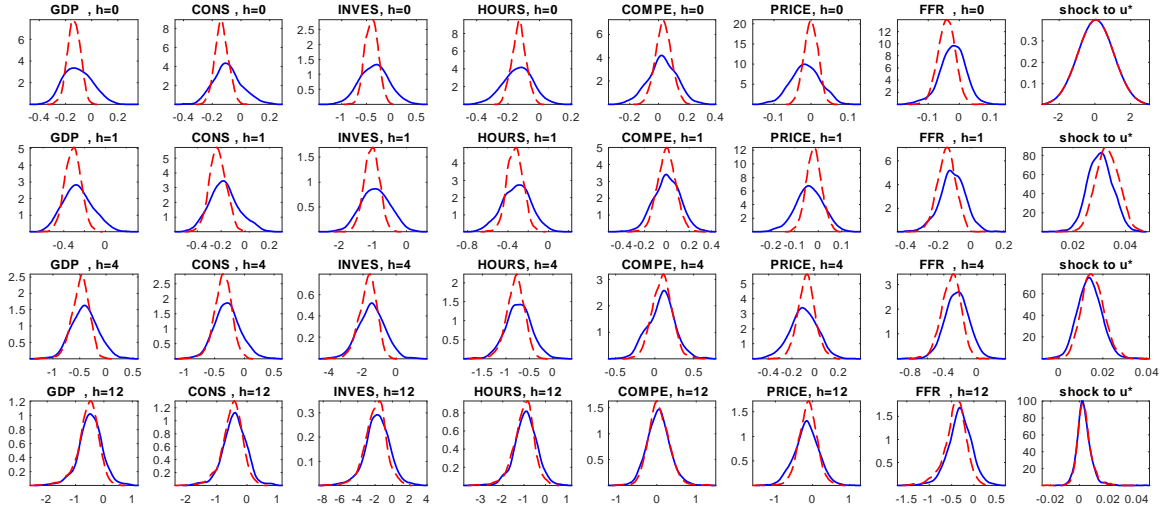


Figure 18: Financial uncertainty shock, quarterly data. Distribution of impulse responses at selected horizons. Blue solid line denotes the case  $\psi \neq 0$ , red dashed line denotes the case  $\psi = 0$ .

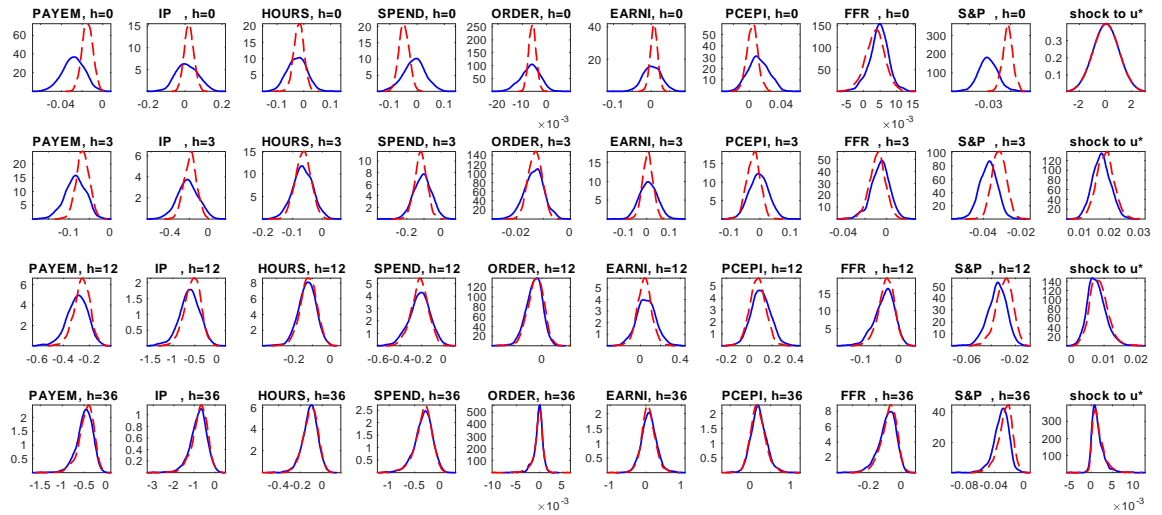


Figure 19: Financial uncertainty shock, monthly data. Distribution of impulse responses at selected horizons. Blue solid line denotes the case  $\psi \neq 0$ , red dashed line denotes the case  $\psi = 0$ .

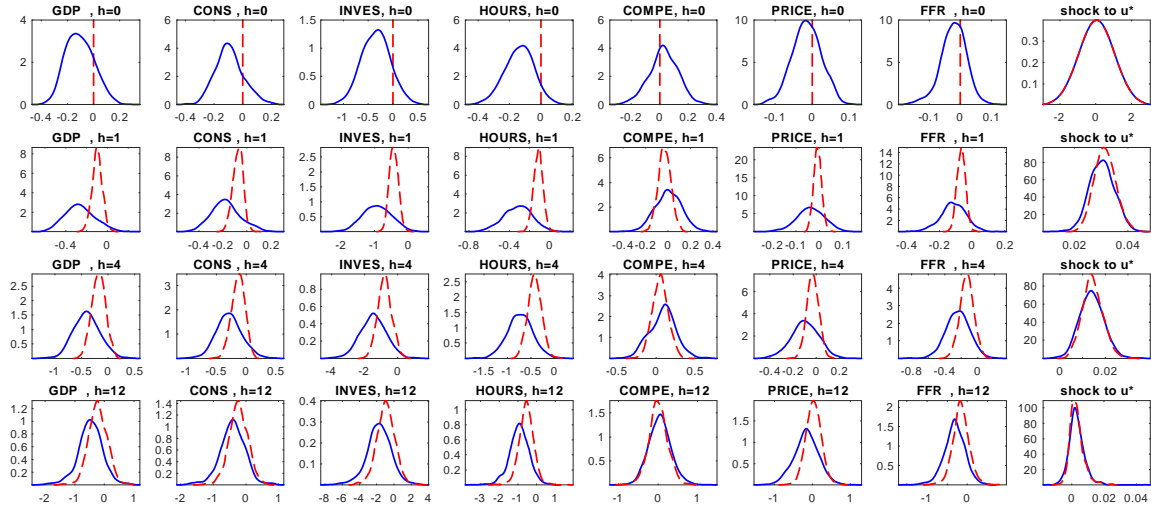


Figure 20: Financial uncertainty shock, quarterly data. Distribution of impulse responses at selected horizons. Blue solid line denotes the case  $\phi \neq 0$ , red dashed line denotes the case  $\phi = 0$ .

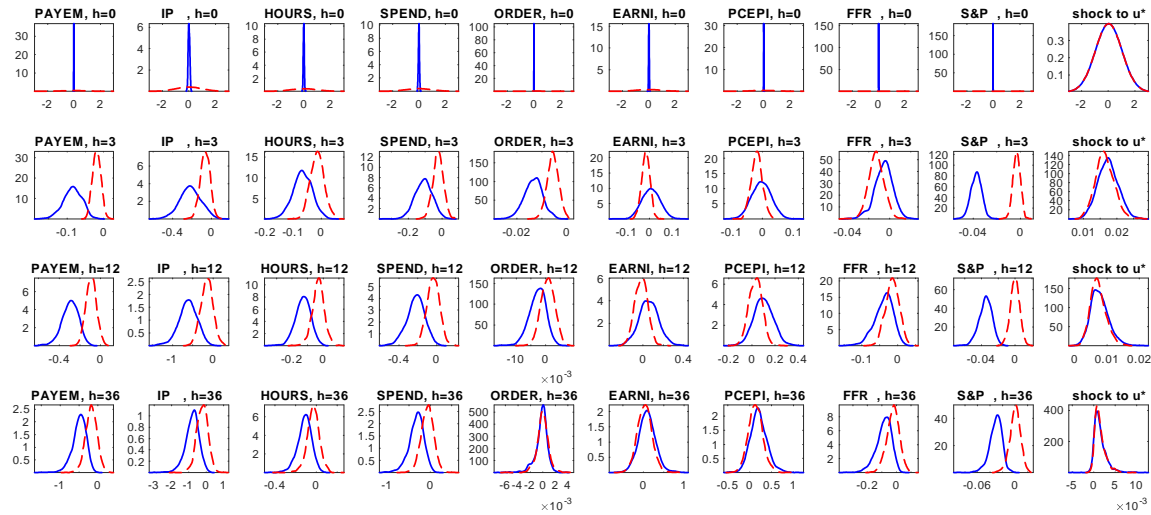


Figure 21: Financial uncertainty shock, monthly data. Distribution of impulse responses at selected horizons. Blue solid line denotes the case  $\phi \neq 0$ , red dashed line denotes the case  $\phi = 0$ .